Liquid Atomization: Vorticity Dynamics and Real-fluid Thermodynamics

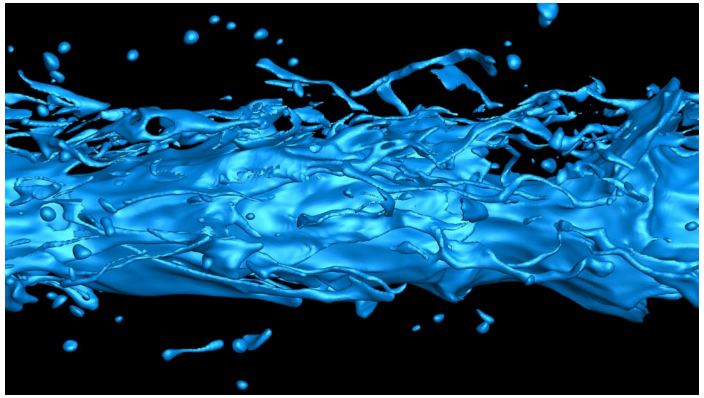

William A. Sirignano University of California, Irvine

Major Contributors

Former PhD students: Dorrin Jarrahbashi, Texas A&M U. ;
Arash Zandian, Tesla; Jordi Poblador-Ibanez, Argonne Labs.
Collaborator: Fazle Hussain, Texas Tech U.; Pavel Popov, SDSU
Funding sources: NSF, US ARO, XSEDE Supercomputer

High Reynolds-number, high Weber-number domain.

Transitional turbulence with need for direct numerical simulation (DNS).

Vortex dynamics can explain well the controlling physics for atomization.

High pressures, transcritical behavior, real-fluid thermodynamics.

Governing Equations for Incompressible, Viscous Newtonian Fluid Flow

- Continuity: $\nabla . \vec{u} = 0$ (incompressible)
- Level-set equation: $\frac{\partial \theta}{\partial t} + \vec{u} . \nabla \theta = 0$
- $D = \frac{1}{2}[(\nabla \vec{u}) + (\nabla \vec{u})^T]$
- Navier-Stokes: $\frac{\partial (\rho \vec{u})}{\partial t} + \nabla . (\rho \vec{u} \vec{u}) = -\nabla p + \nabla . \left(2\mu \vec{D}\right) + \vec{F}_\sigma$

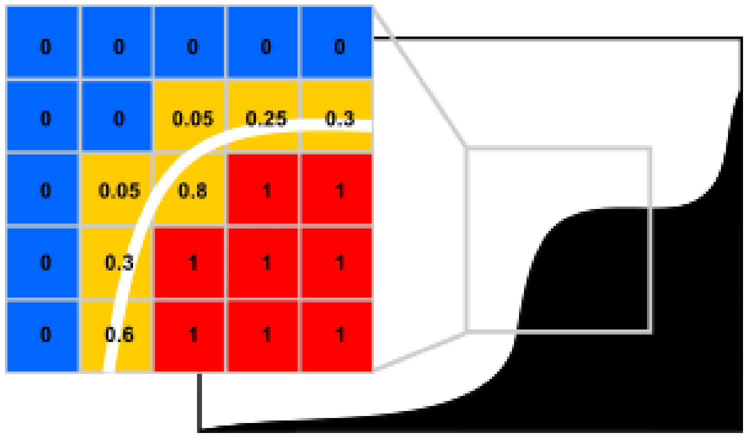

Interface Tracking

Temporal Instability **Spatially Developing Jet**

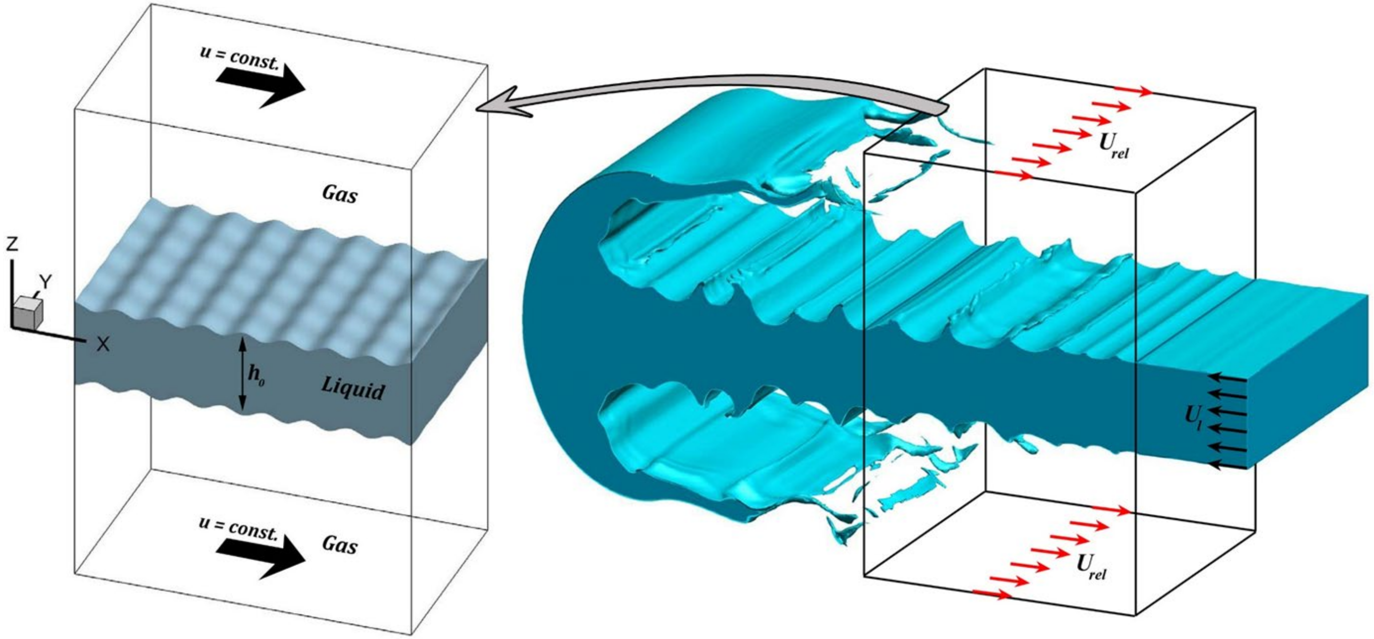

Key Dimensionless Groups

$$Re = \frac{\rho_l U h}{\mu_l}, \quad We = \frac{\rho_l U^2 h}{\sigma}$$

$$\hat{\rho} = \frac{\rho_g}{\rho_l}, \quad \hat{\mu} = \frac{\mu_g}{\mu_l}, \Lambda = \frac{\lambda}{h}$$

Round jets and unstable vortex rings

Axisymmetric vortex rings develop 3D instabilities

Liepmann & Gharib (1992), water-into-water

Well established theory indicates that hairpin vortices form.
The hairpins from the braid overlap with hairpins from the ring.

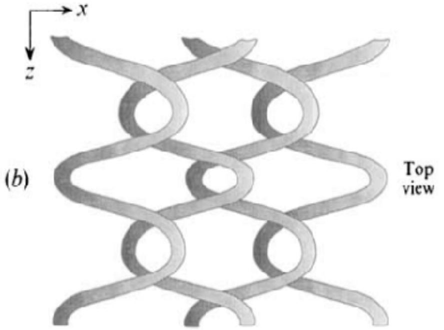

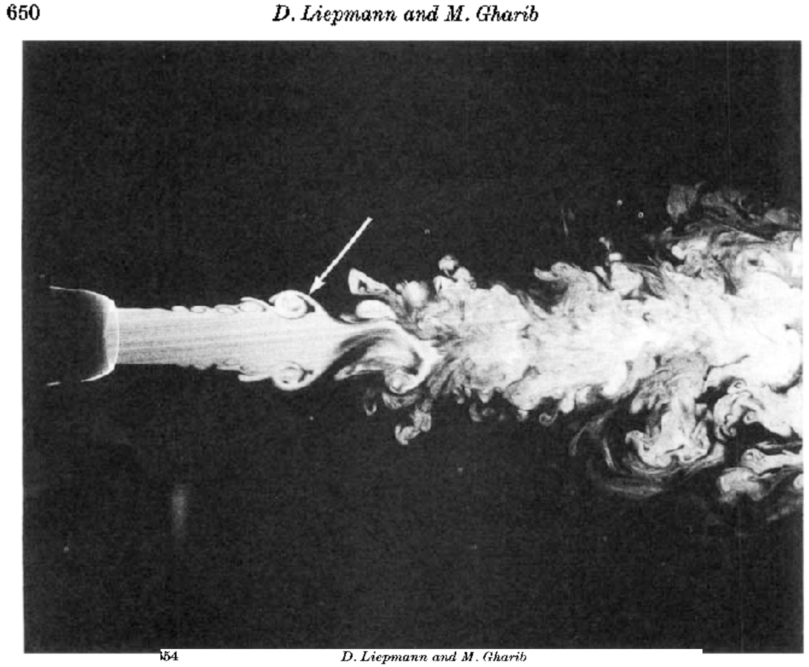

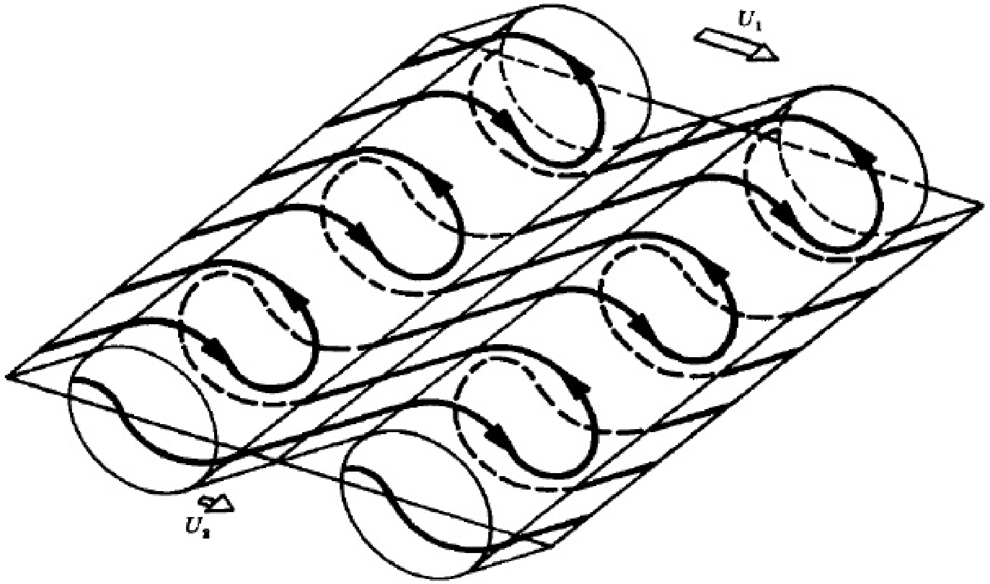

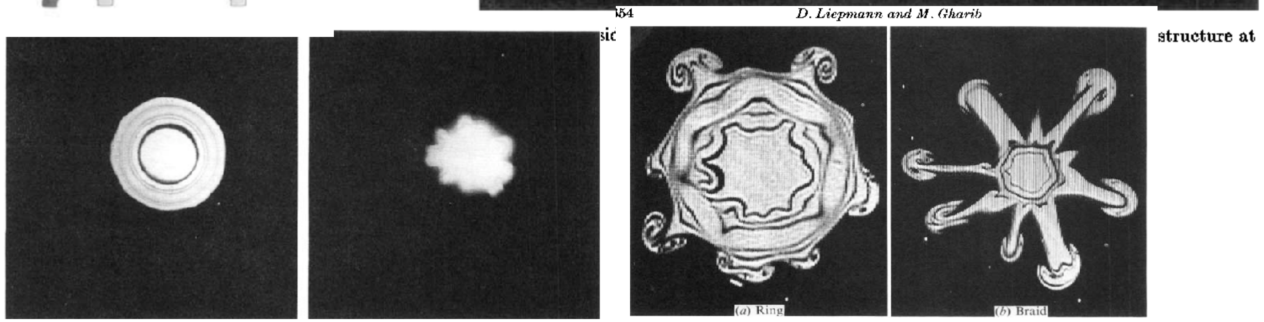

Ring **Braid** **Ring** **Braid**

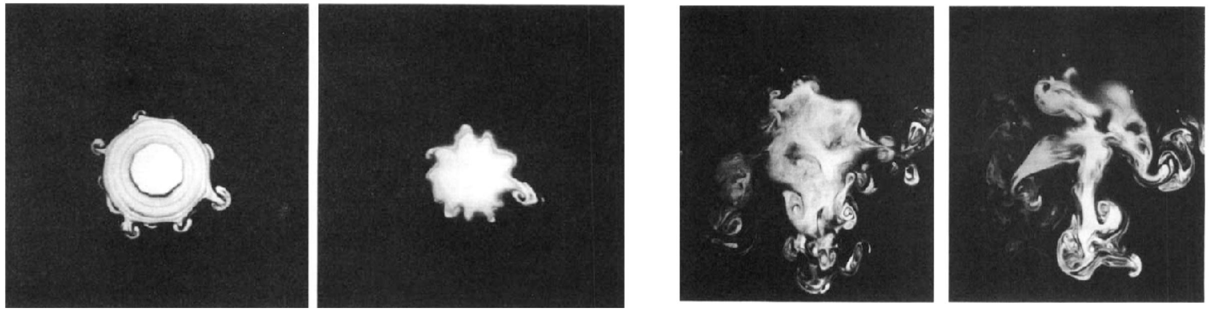

Liquid jet with co-axial air

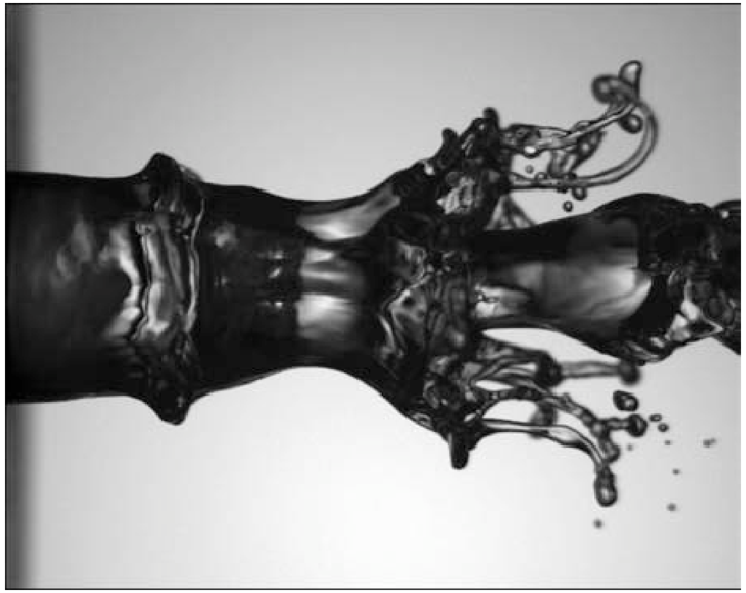

Marmottant & Villermaux (2004)

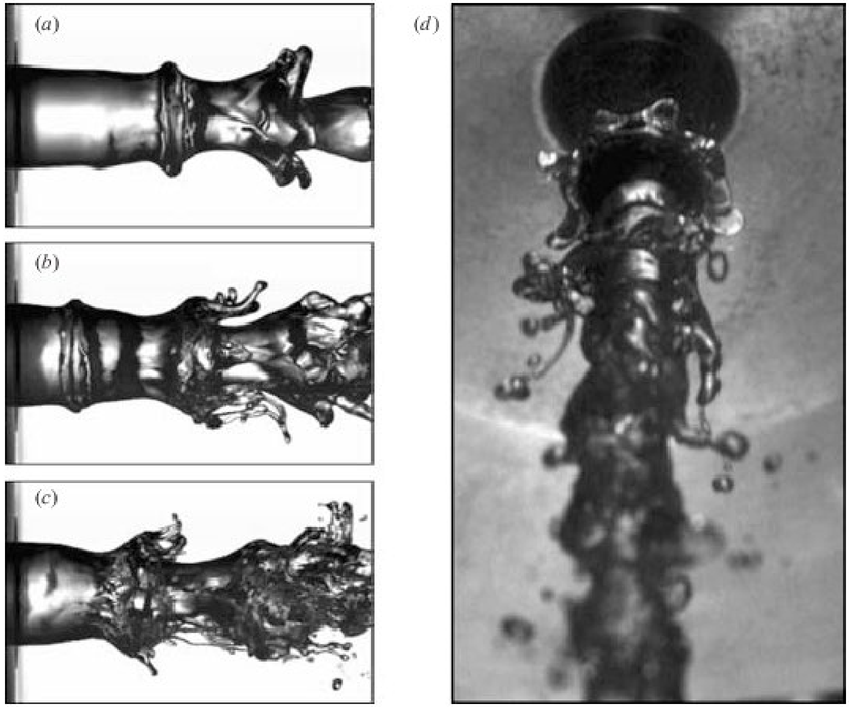

-- Cones form.

-- Azimuthal lobes form on cones with attribution to Rayleigh-Taylor instability.

-- Ligaments form in time from lobes.

-- This experimental finding is consistent with our Domain I analytical results.

Different atomization cascades occur depending on We, Re, density and viscosity ratios

Lobes, Ligaments, Droplets

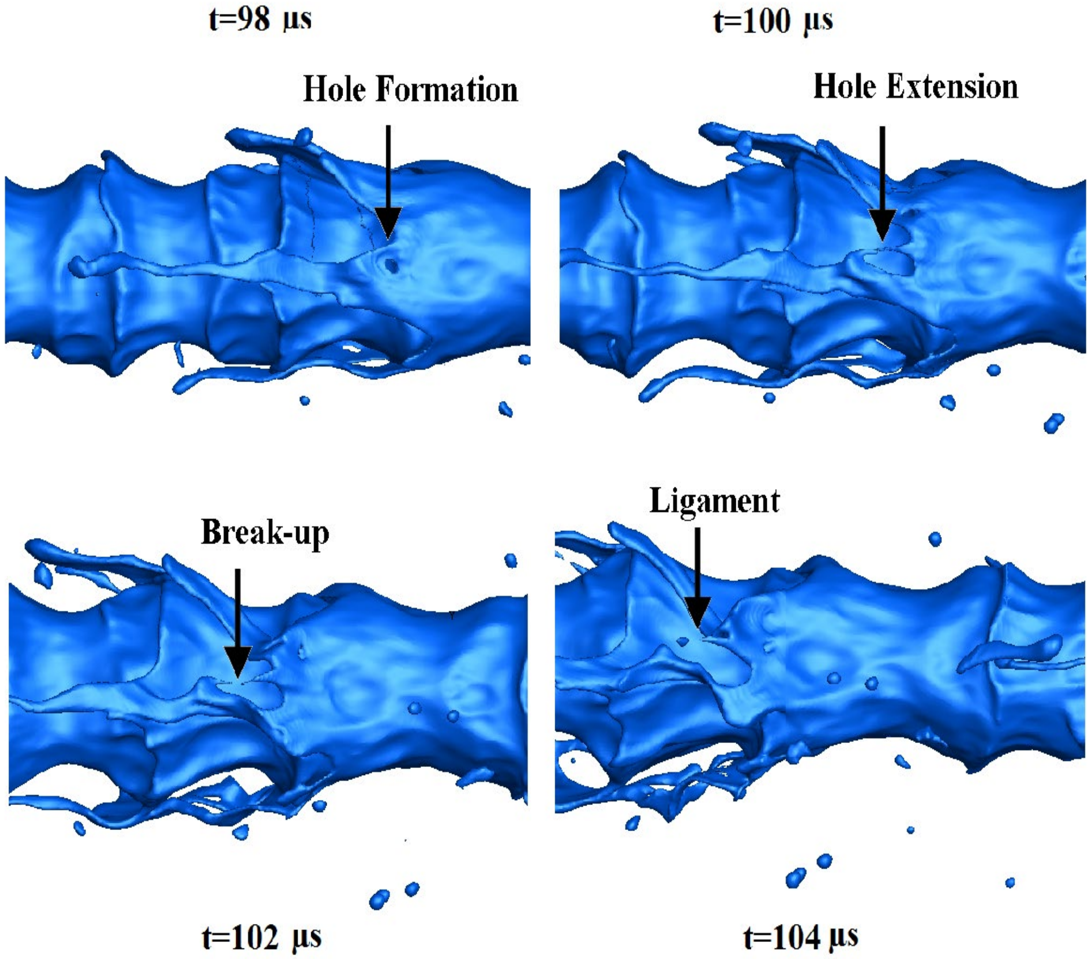

Lobes, Holes, Bridges, Ligaments, Droplets

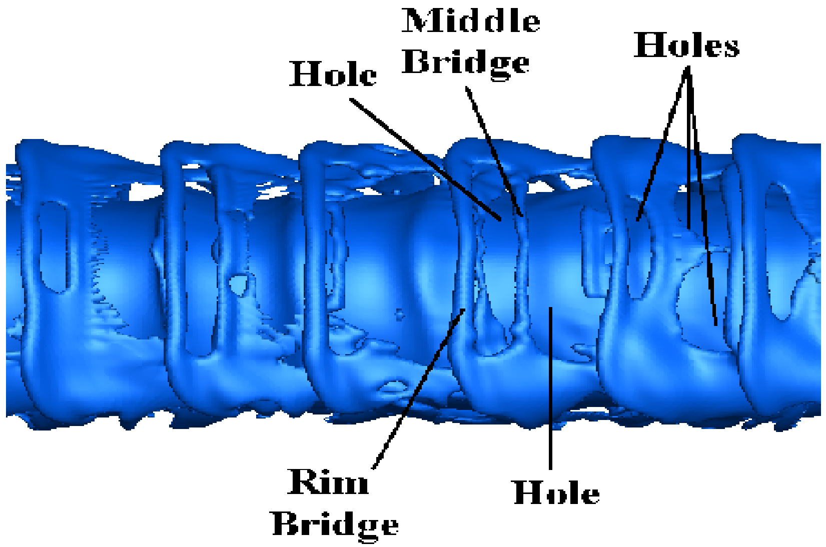

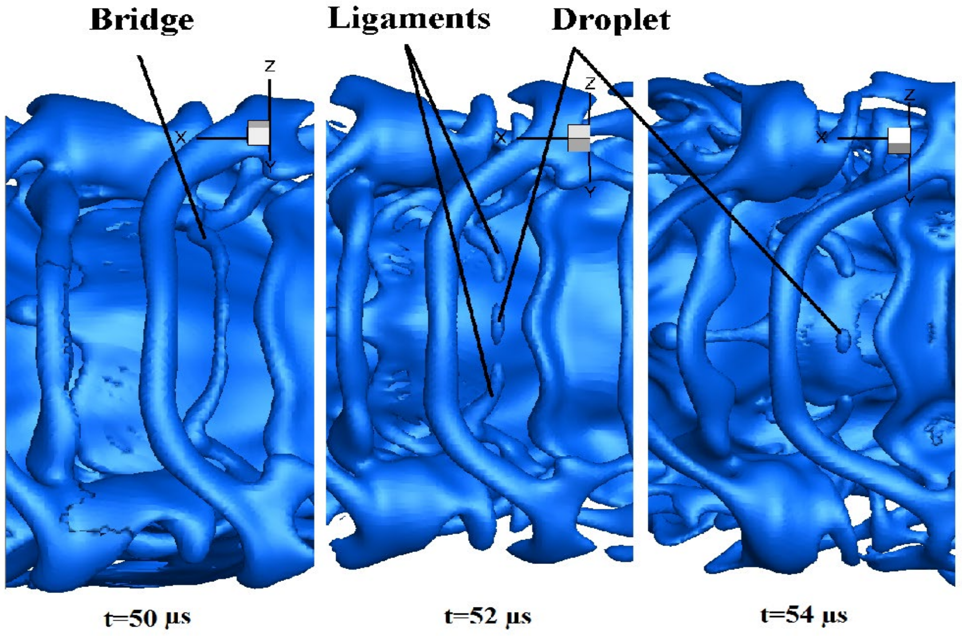

Spatially Developing Liquid Jets Show Similar Breakup Mechanisms to Temporally Unstable Jets

Time →→→

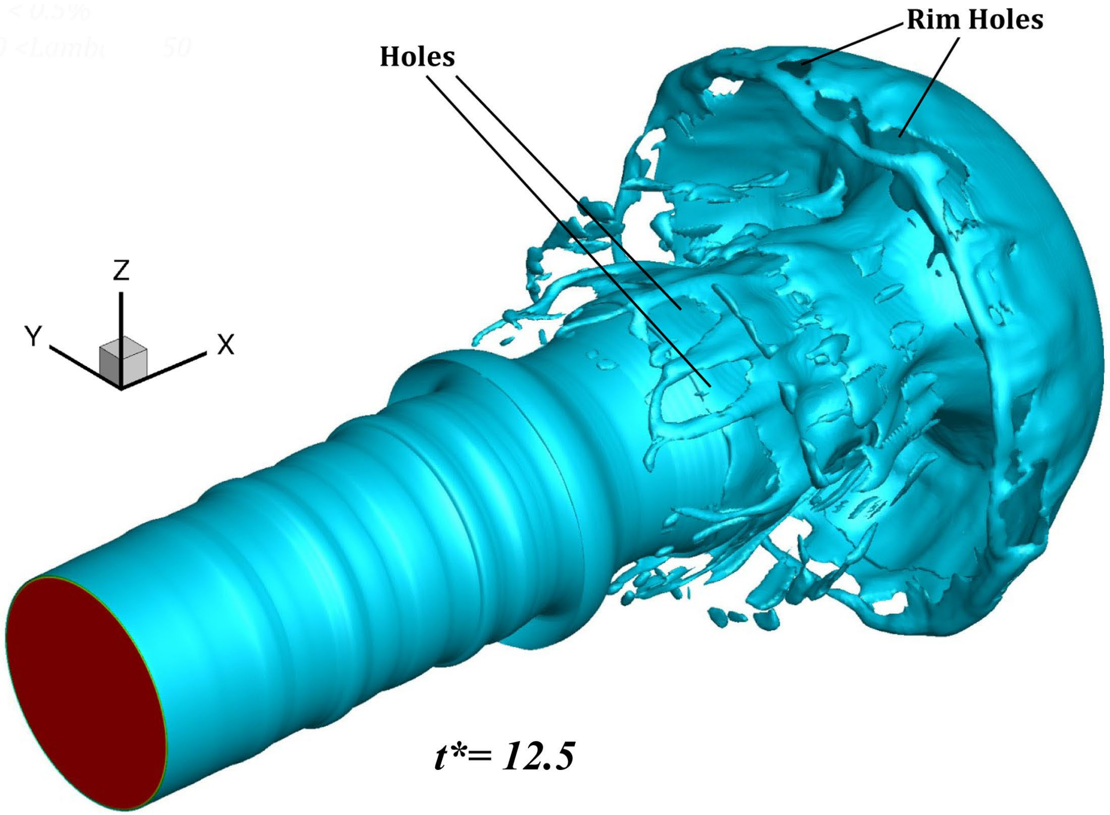

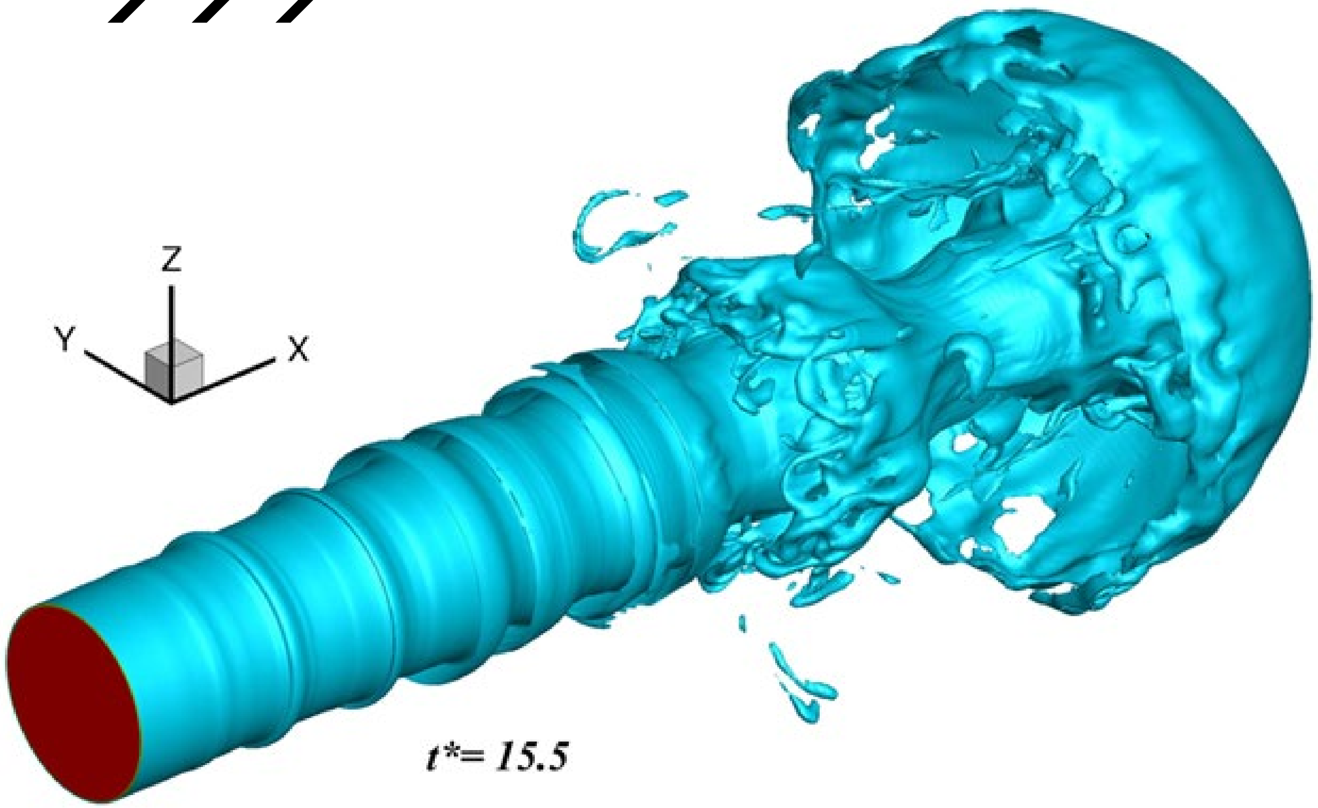

It is reasonable to study the physics of atomization mechanisms using temporally unstable flows.

Wavelength Analysis on Unstable Liquid Jet

K-H waves form cones, azimuthal R-T waves form on cones, ligaments result from R-T waves, capillary action plus more R-T waves on ligaments.

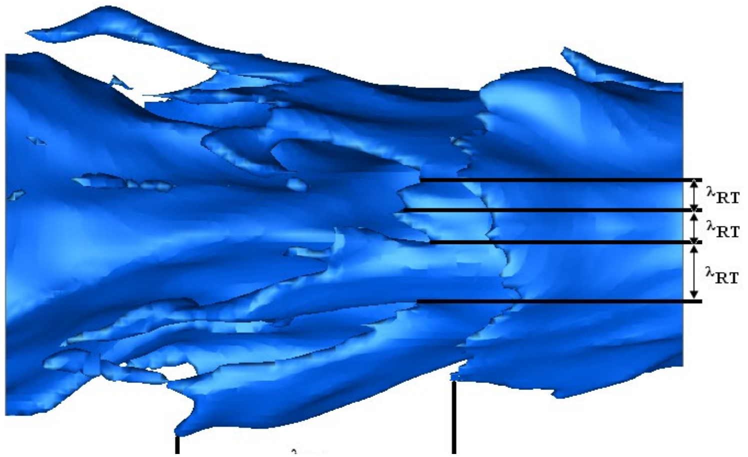

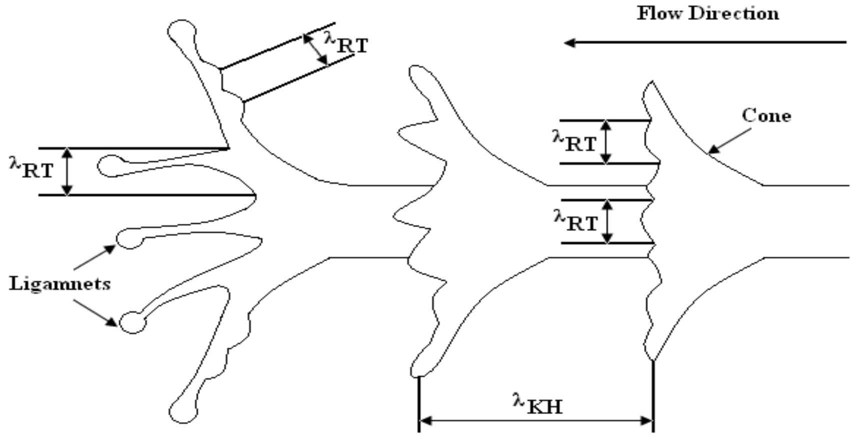

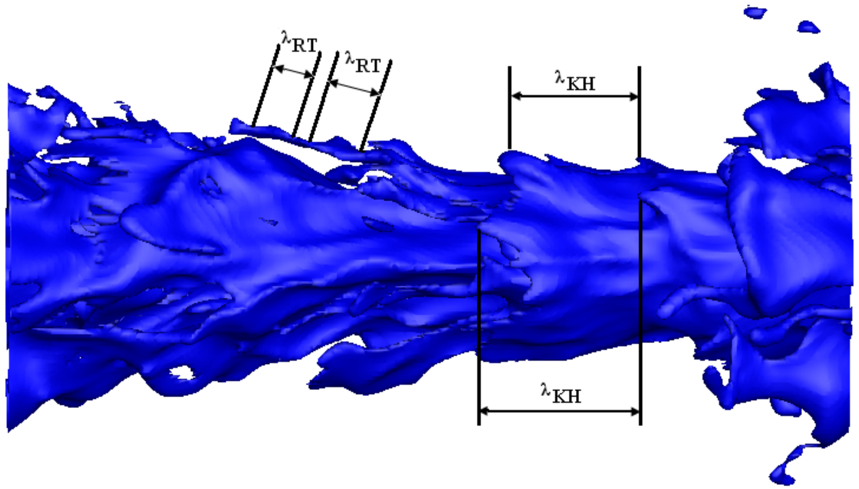

- **R-T instability wavelengths on the ligaments vary between 15-50 µm.**
- **Transverse R-T instability wavelengths on the crests varies between 20 to 70 µm.**
- **Acceleration is the main factor to develop the R-T instability on the ligaments and crests .**

Three Domains based on Re_{liquid} and We_{gas}

Domain I
Lobe-Ligament-Droplets
Low Re_l , low We_g

Domain II
Lobe-Hole-Bridge-Ligament-Droplets
High We_g

Domain III
Lobe-Corrugations- Ligament-Droplets
High Re_l , low We_g

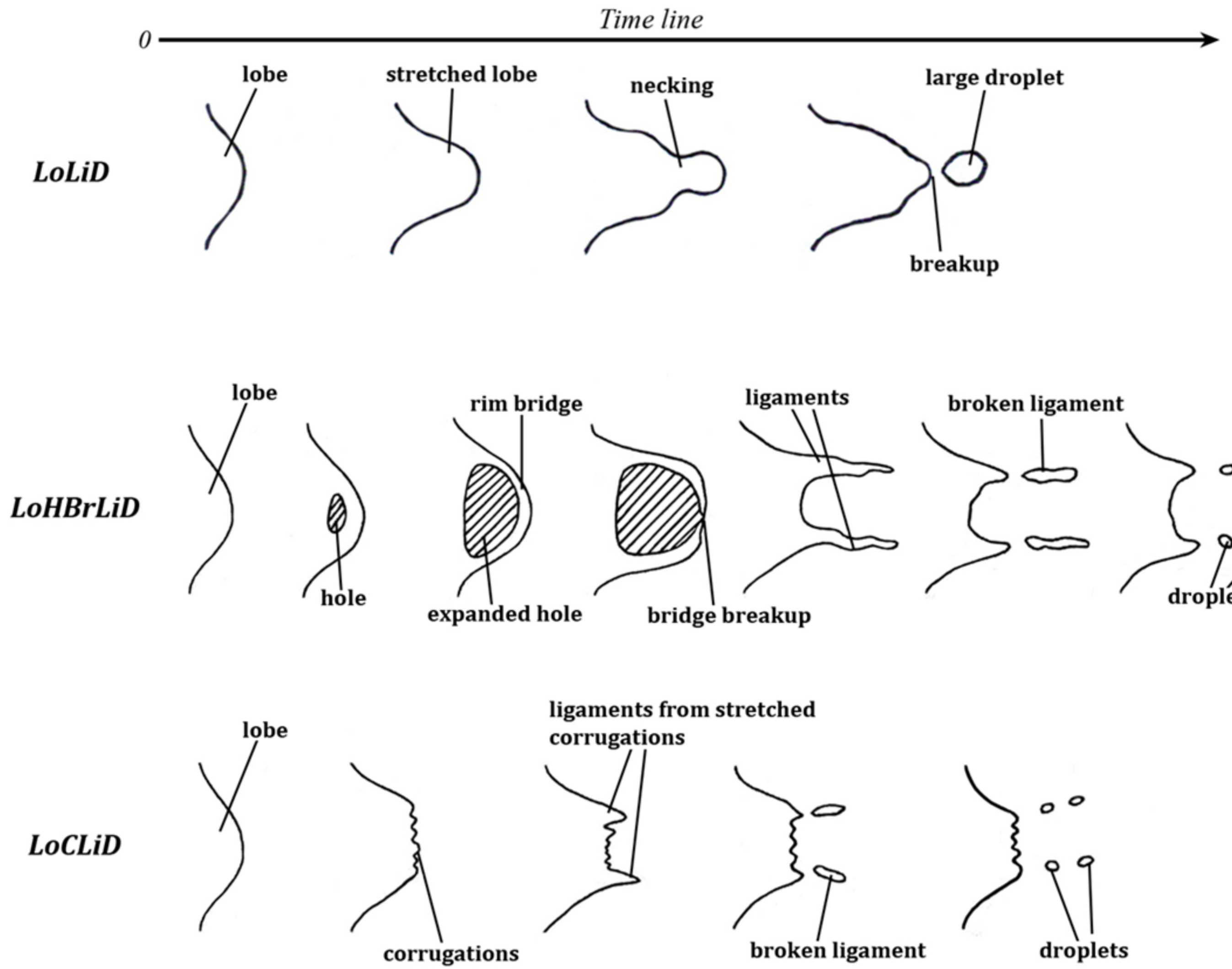

Interface Development in Three Domains

Domain I
Lobe-Ligament-Droplets
Low Re_l , low We_g

Domain II
Lobe-Hole-Bridge-Ligament-Droplets
High We_g

Domain III
Lobe-Corrugations-Ligament-Droplets
High Re_l , low We_g

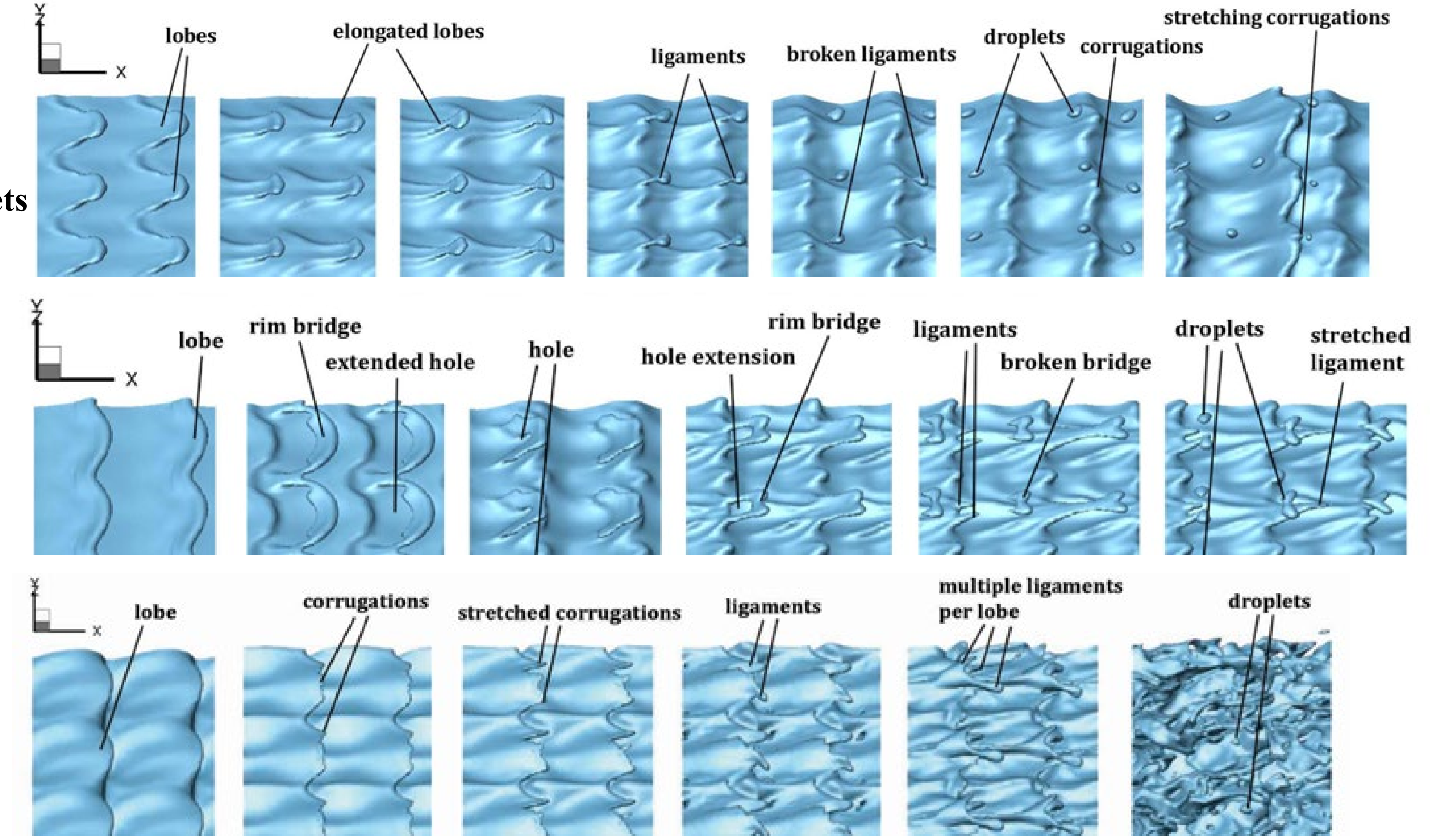

Three Domains for Round Jets

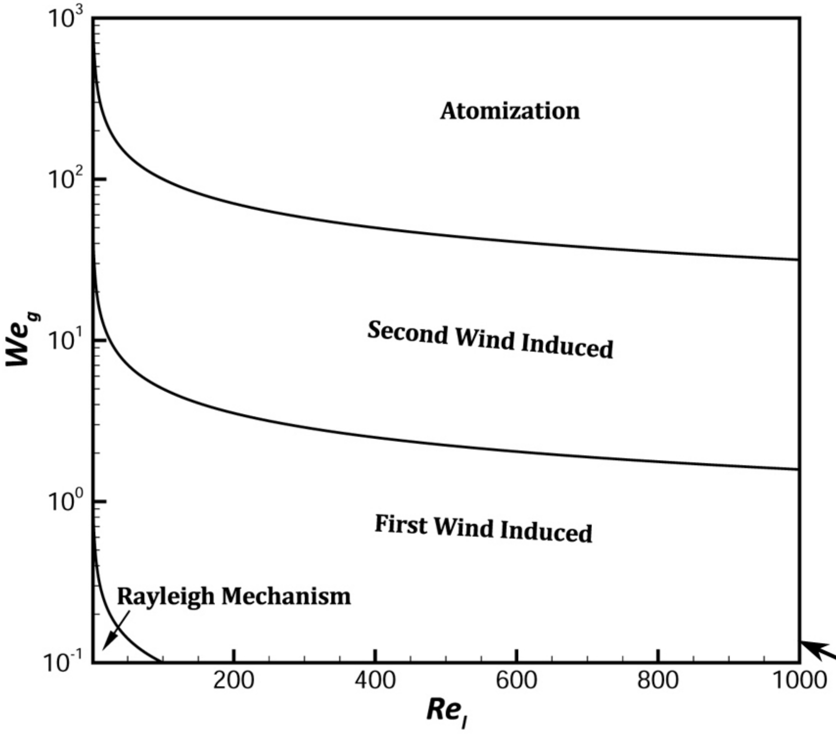

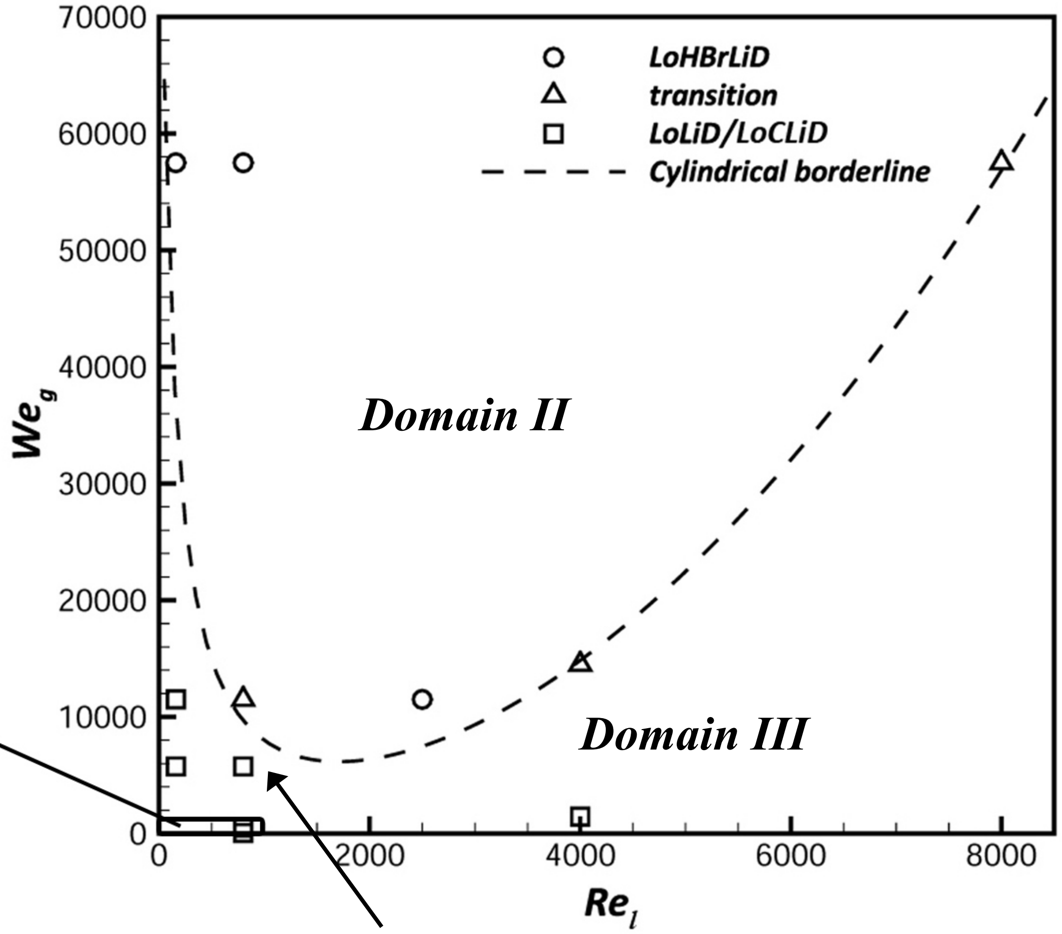

Domain I

Three Domains for Planar Jets with different density ratios

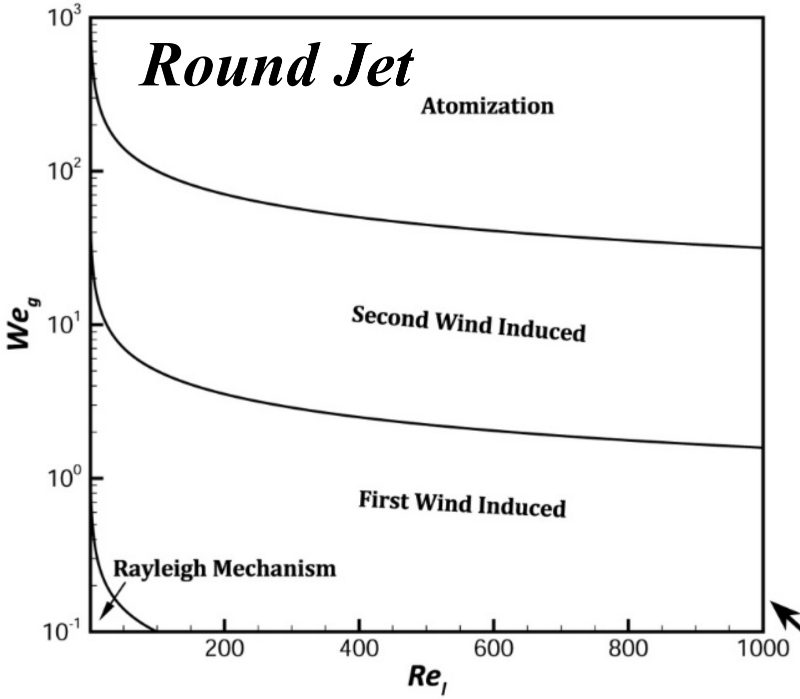

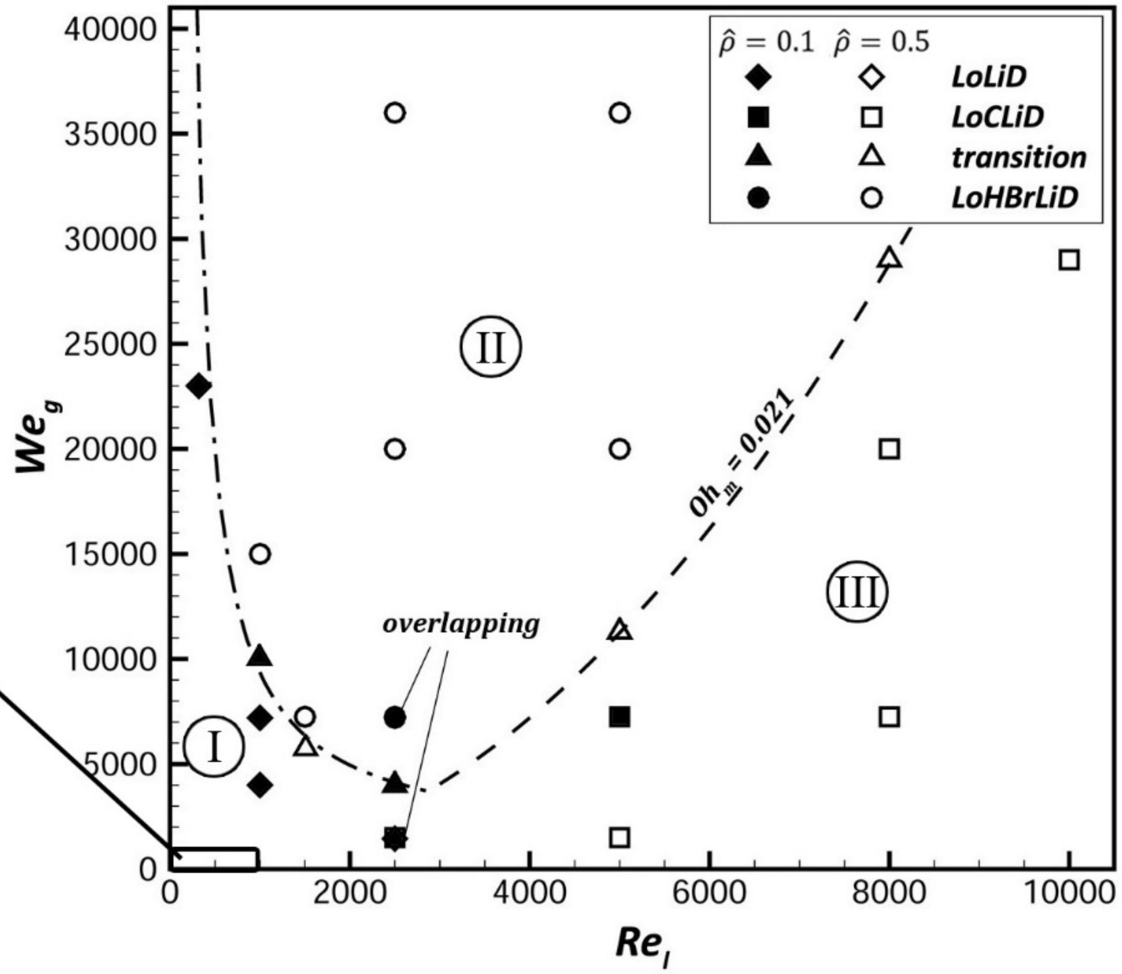

Modified Ohnesorge number $Oh_m = (Re_l)^{1/2} / We_g$

Boundary along $We_g = A/Re_l + B^2 Re_l^2 + C$

For large Re_l, $We_g \sim B^2 Re_l^2$ *or constant* Oh_m

Vorticity

Schowalter (1994): Baroclinic torque forms vortex sheets along an unstable interface.

As a vortex rolls up, concentrating vorticity, centrifugal force creates a pressure minimum near the vortex center. This local minimum of pressure can be used to detect vortex structures.

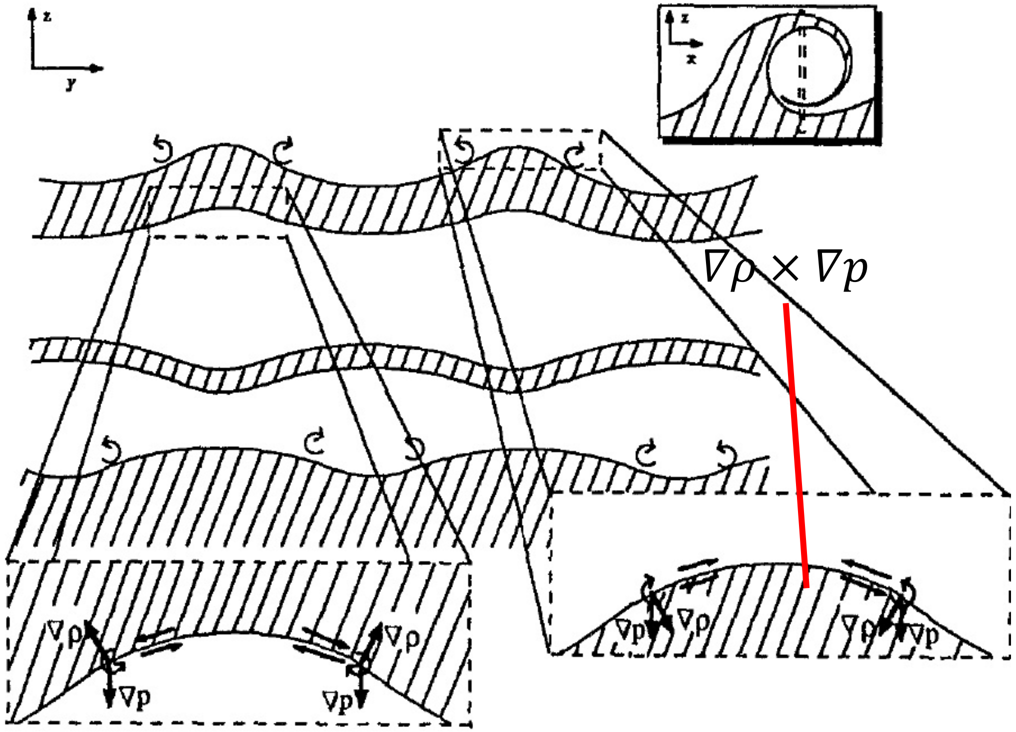

A pressure minimum in a plane implies that two second derivatives of pressure are positive.

However, other things can cause regions of minimum pressure: viscous stress, tension, unsteady effects. Thus, we aim to focus on inertial effects in minimizing pressure. F. Hussain and co-workers have provided an analytical post-processing technique based on this minimization principle.

Vortex Identification Method

Constant-density λ_2 Method, Jeong & Hussain, 1995

Variable-density λ_ρ Method, Yao & Hussain, 2018

$$\frac{D}{Dt}(\rho u_i)_{,j} + (\rho u_i)_{,k}u_{k,j} + (\rho \Theta u_i)_{,j} = -p_{,ij} + \tau_{ik,kj} \qquad \Theta = \boldsymbol{\nabla}\cdot\boldsymbol{u} = u_{k,k}$$

$$\frac{DS^m_{ji}}{Dt} - S^\tau_{ij} + S^M_{ij} + S^\Theta_{ij} = -p_{,ij}$$

$$S^m_{ij} = \tfrac{1}{2}[(\rho u_i)_{,j} + (\rho u_j)_{,i}]$$

$$S^\tau_{ij} = \tfrac{1}{2}[\tau_{ik,kj} + \tau_{jk,ki}]$$

$$S^M_{ij} = \tfrac{1}{2}[(\rho u_i)_{,k}u_{k,j} + (\rho u_j)_{,k}u_{k,i}]$$

$$S^\Theta_{ij} = \tfrac{1}{2}[(\rho \Theta u_i)_{,j} + (\rho \Theta u_j)_{,i}]$$

We seek the eigenvalues of approximate the pressure Hessian

$$p_{,ij} \approx -S^M_{ij} - S^\Theta_{ij}$$

In particular, locations with two positive eigenvalues are sought.

Lobe stretching (Domain I, low Re_l, low We_g)

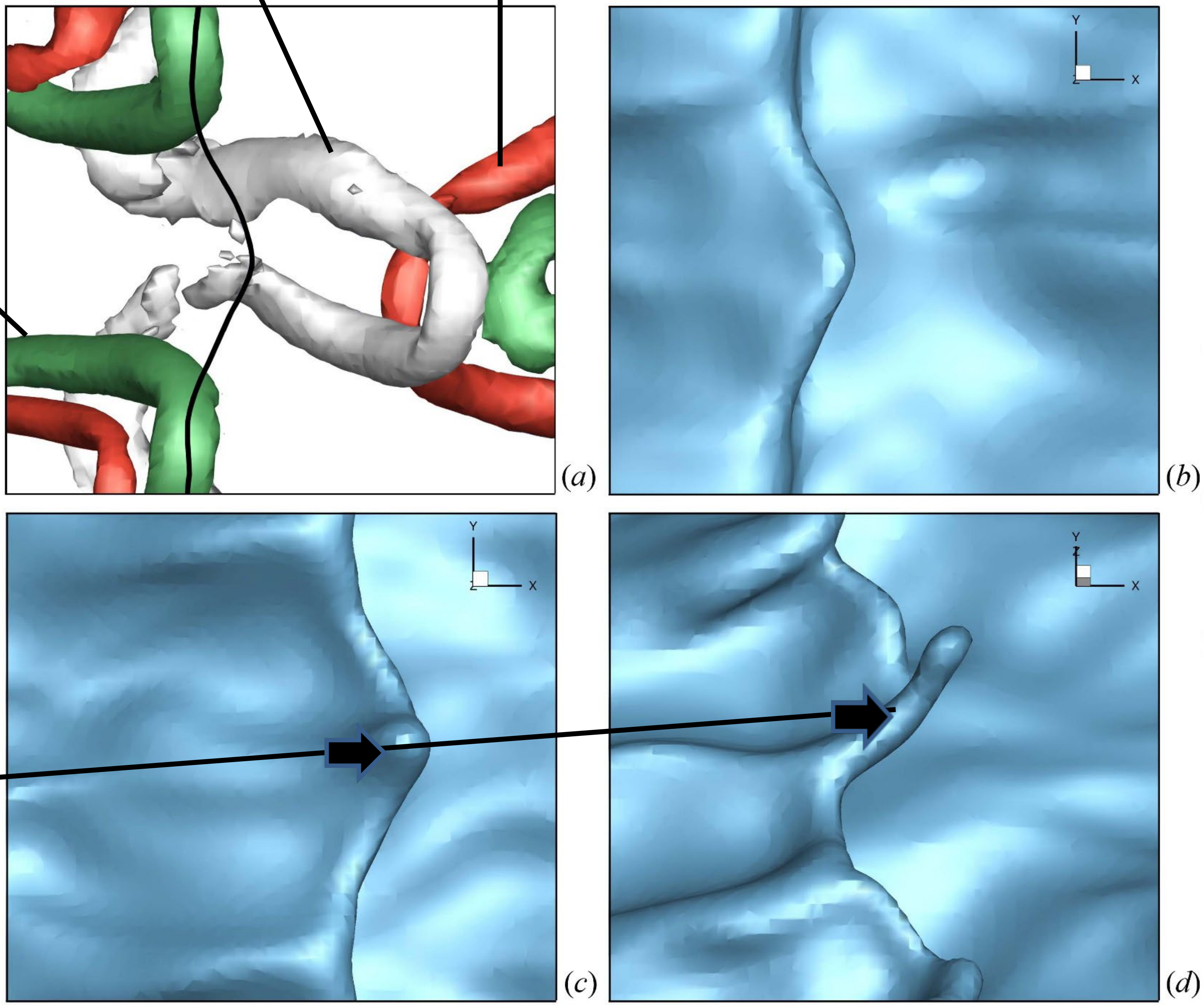

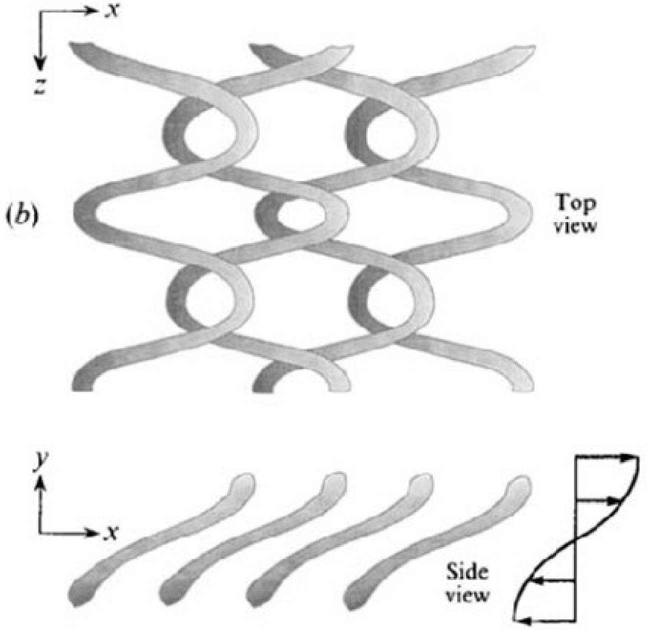

Lobe stretching (Domain I, low Re_l, low We_g)

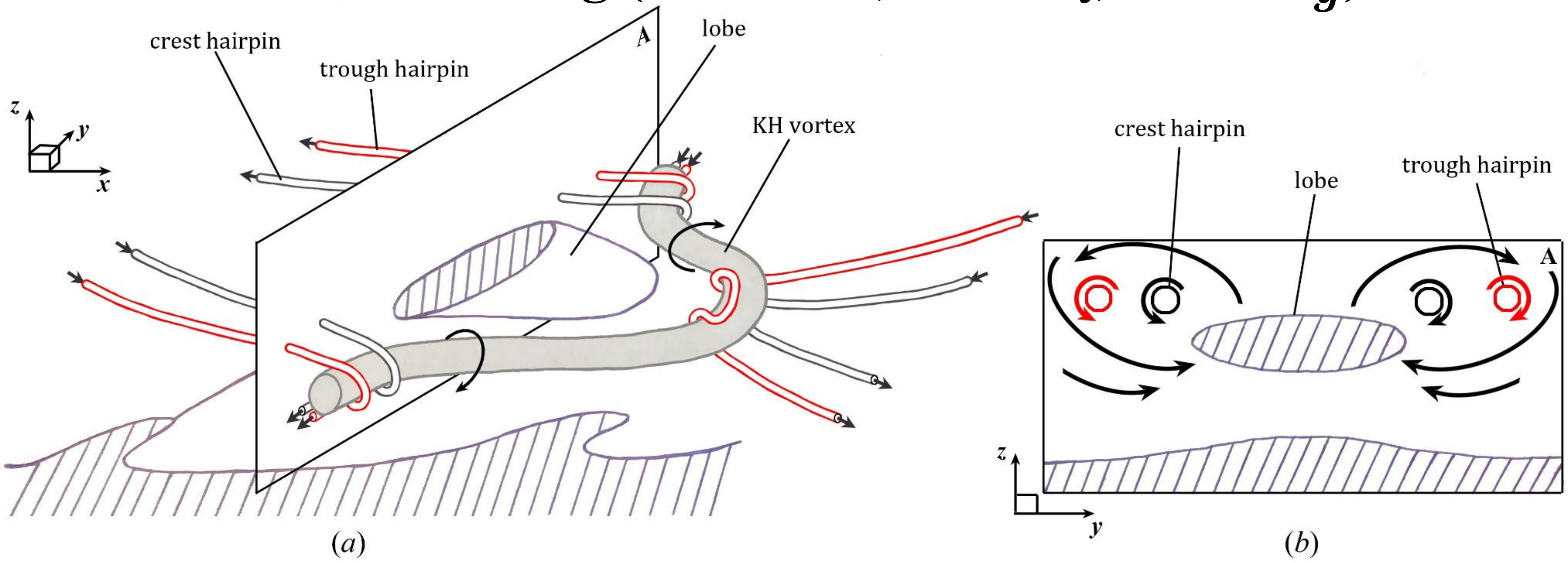

- **KH vortex departs from liquid surface and advects downstream into the gas**
- **Hole formation inhibited because of high surface tension**
- **Small scale corrugations damp because of high viscosity**
- **Two pairs of counter-rotating hairpins wrap around KH vortex**
- **Induced spanwise gas flow squeezes the lobe from sides**

Hole-Bridge formation (Domain II, high We_g)

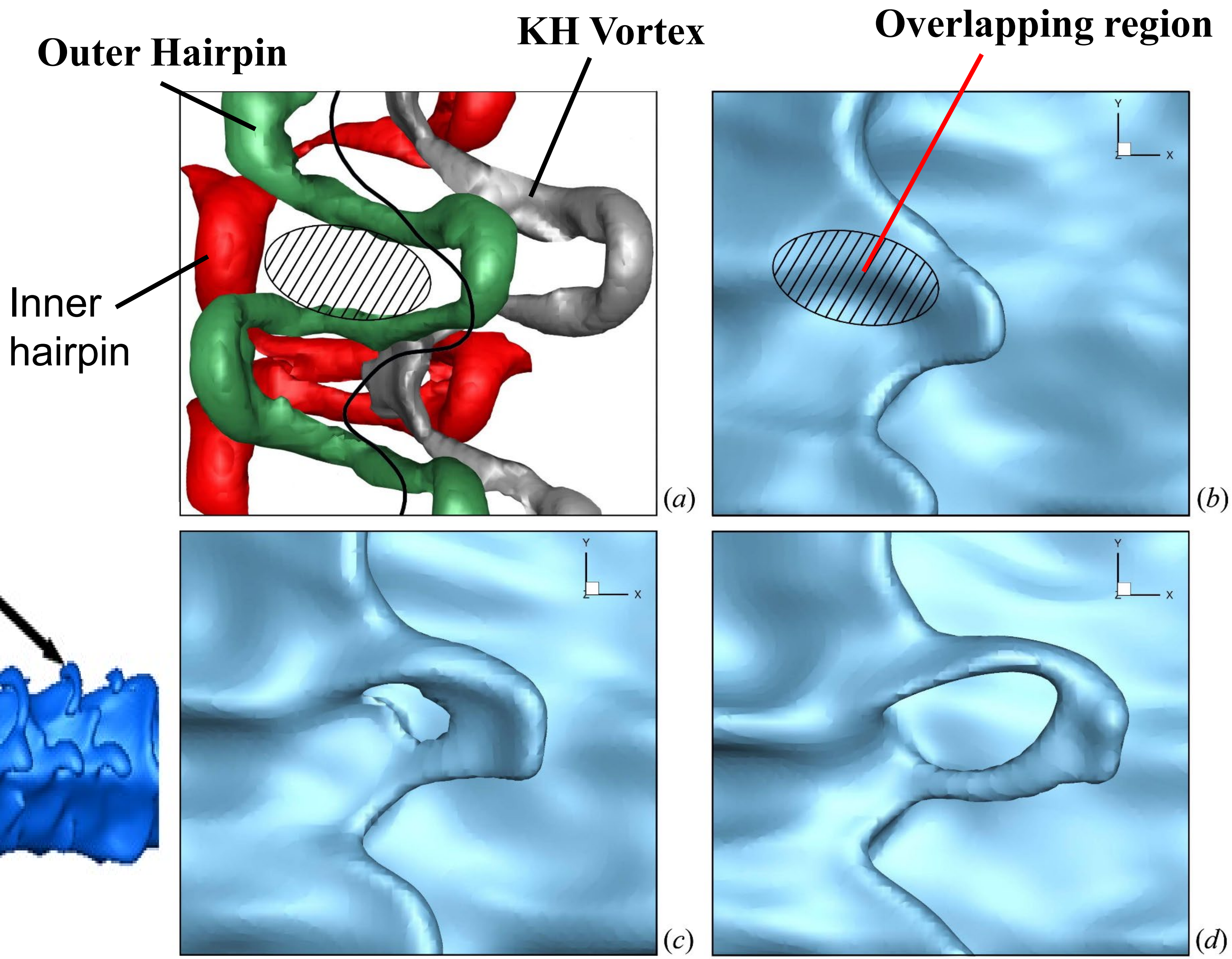

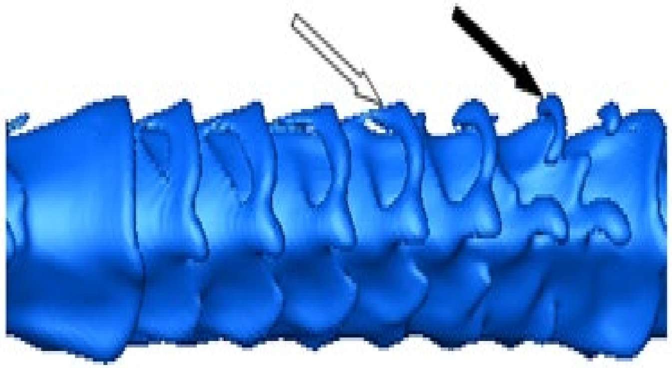

Hole-Bridge Formation (Domain II, high We_g)

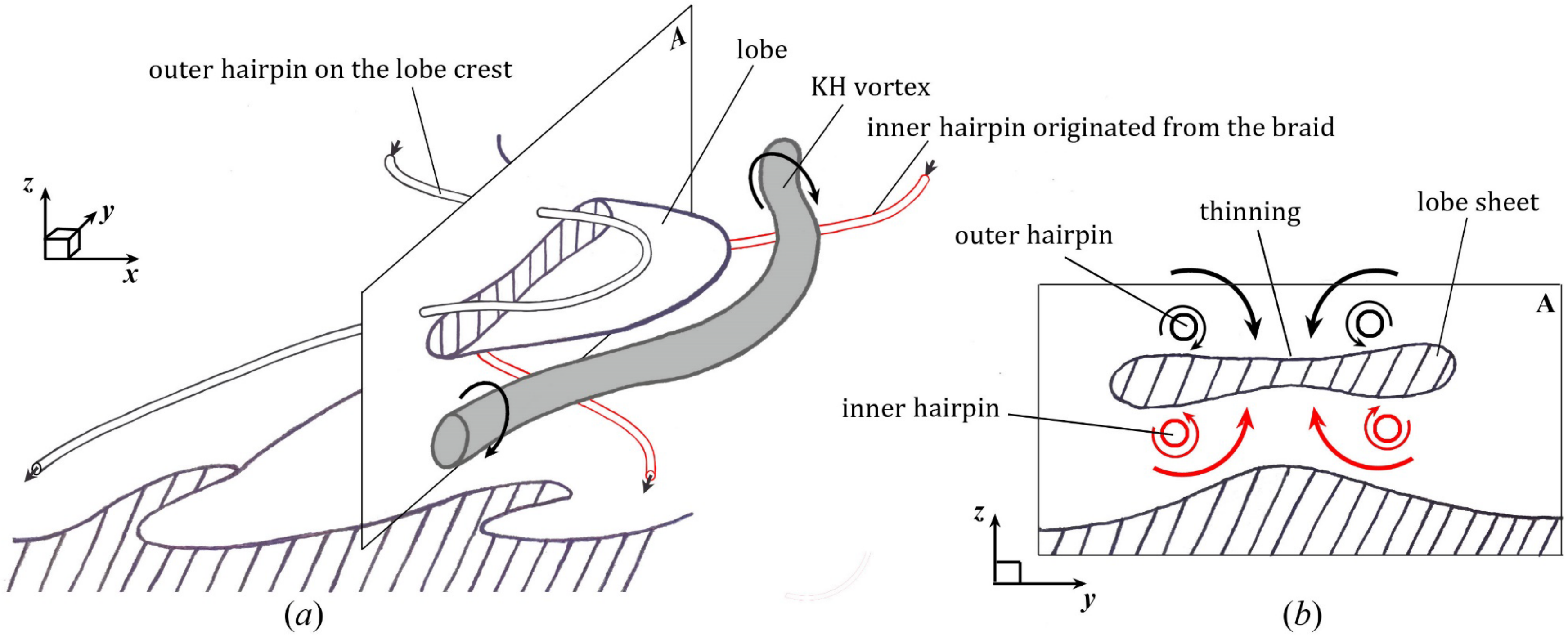

- **Overlapping of oppositely oriented streamwise hairpins occurs on the lobe**
- **The mutual induction of these hairpins thins the lobe at the center**
- **Holes form on the lobes if the surface tension forces are not strong enough to resist perforation (at high We_g)**

Corrugation formation (Domain III, high Re_l)

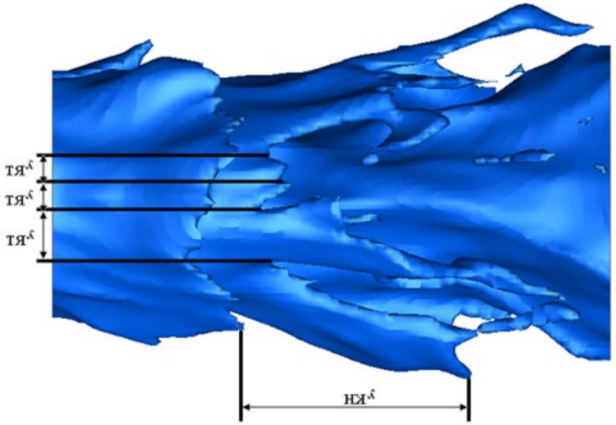

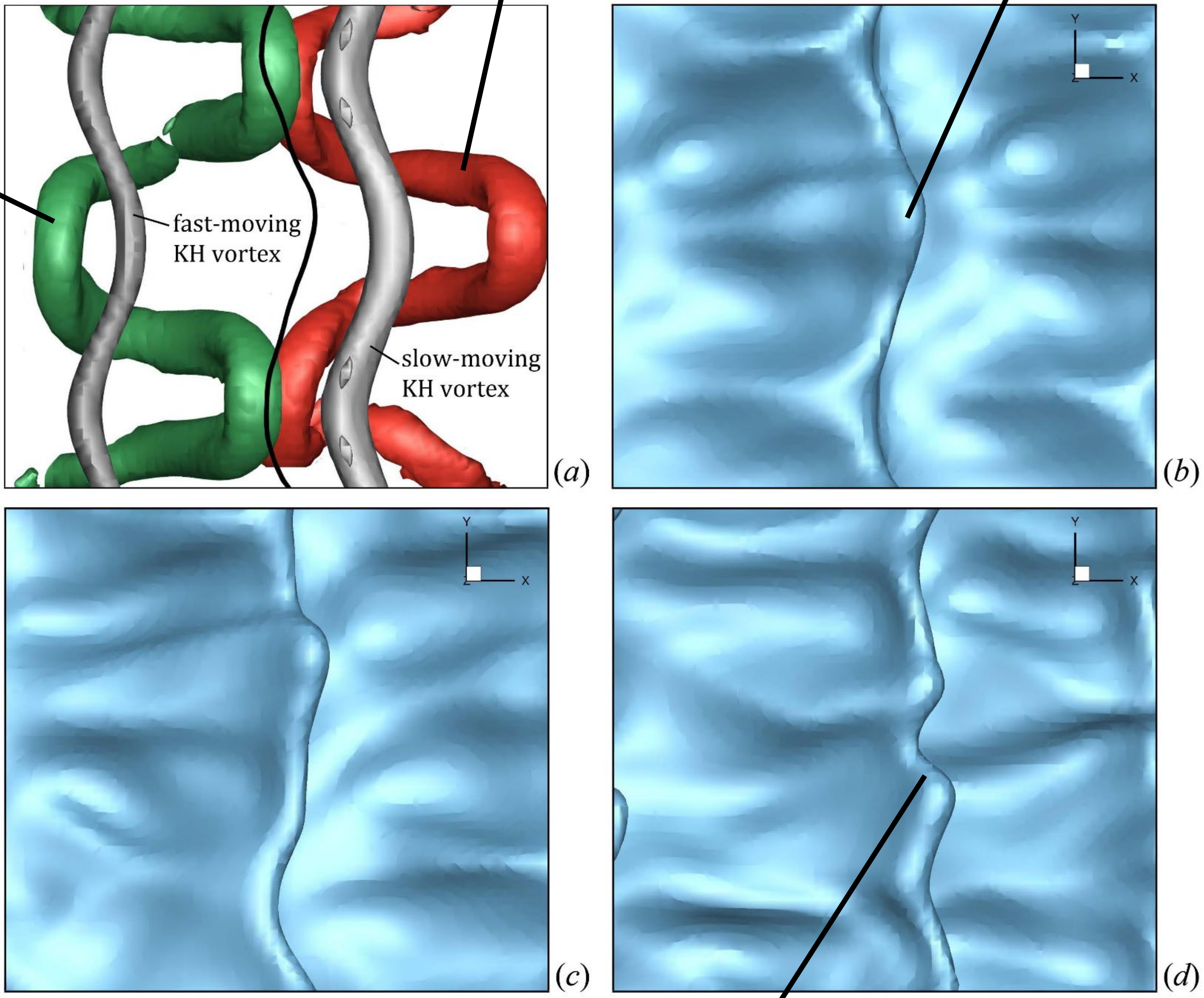

Corrugation Formation (Domain III, high Re_l)

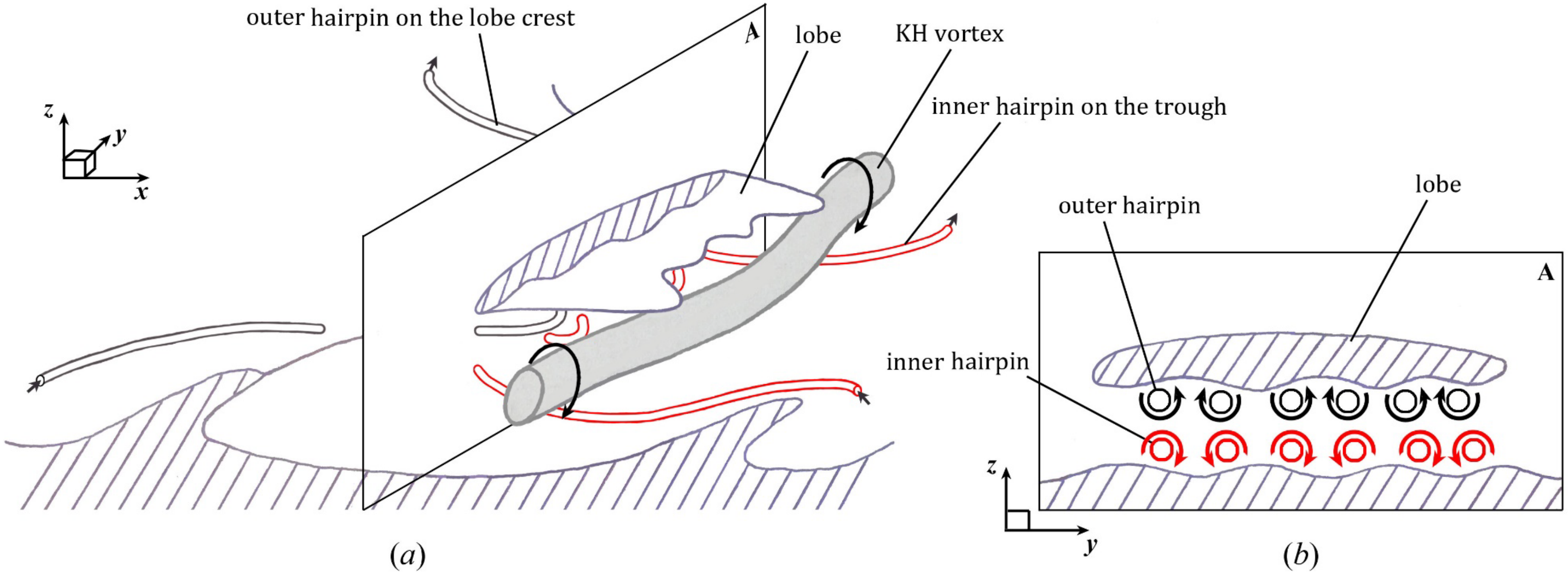

- **Hairpins have more turns, smaller wavelength**
- **Corrugations form on lobe rim following hairpins induction**
- **Corrugations stretch into ligaments**

Mean Spray Width – Temporal Growth

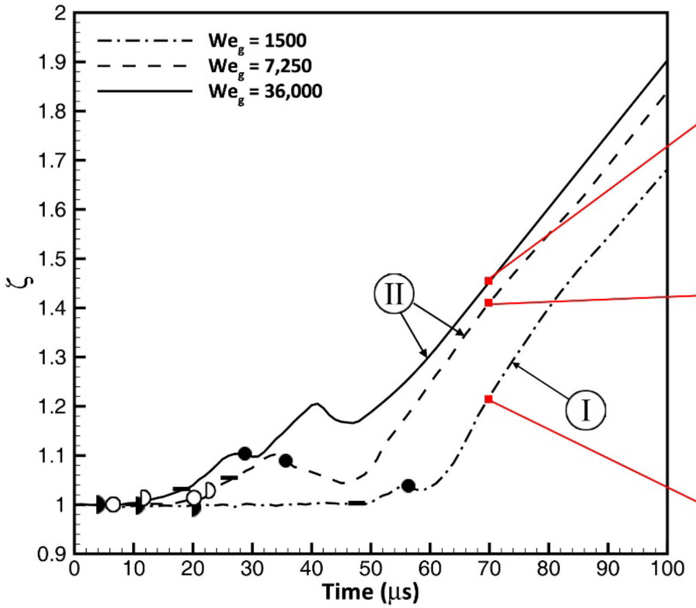

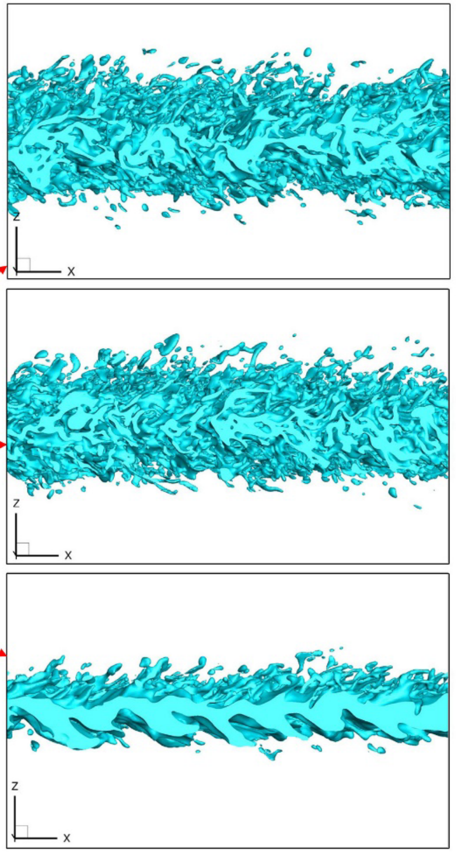

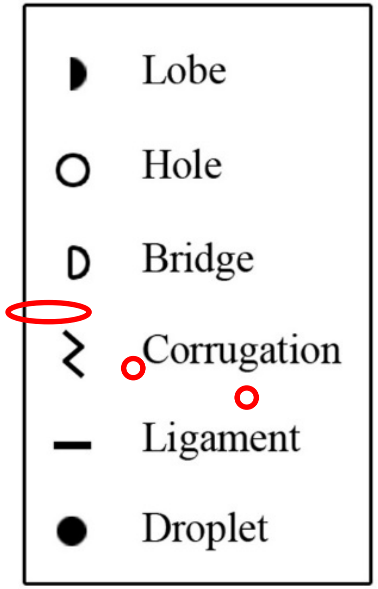

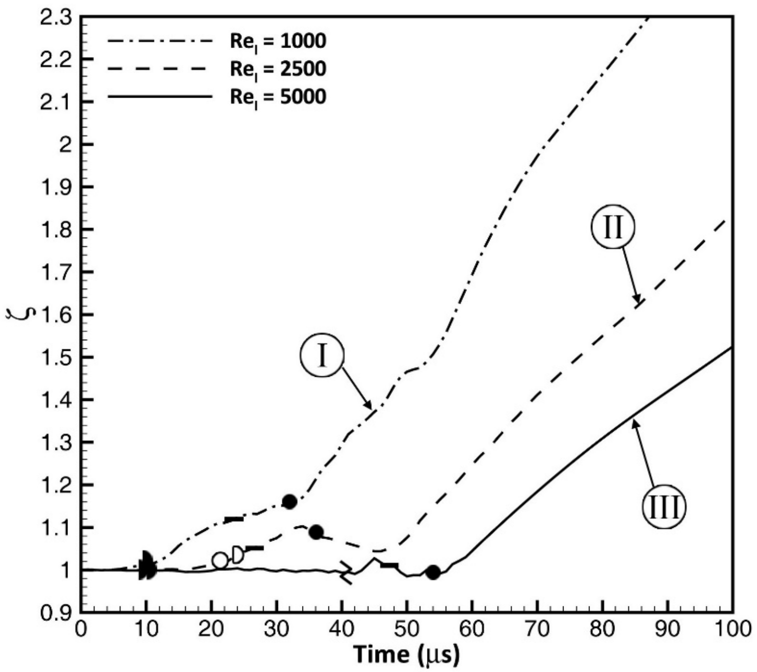

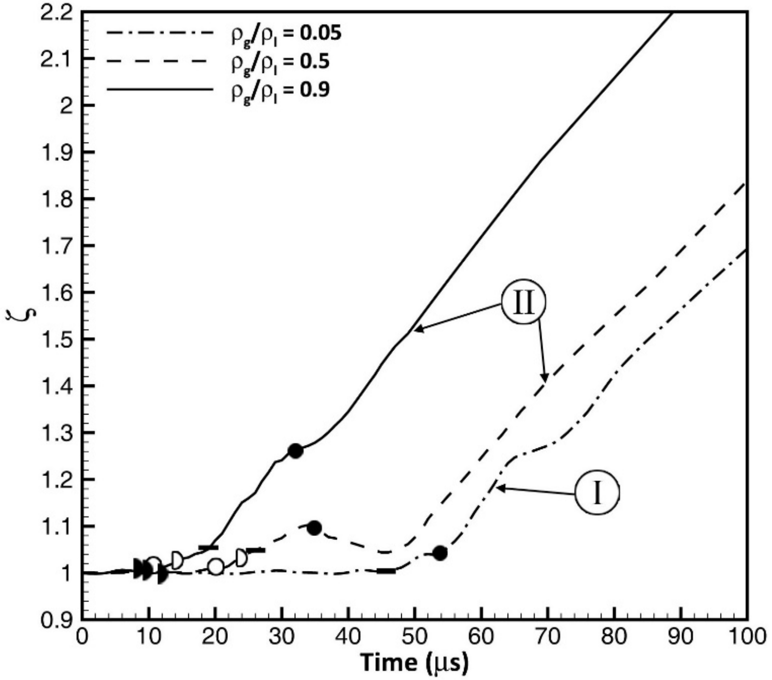

- **Spray spread rate increases with increasing We_g, decreasing Re_l, and increasing $\widehat{\rho}$**
- **Spikes show when the first breakup occurs**
- **Asymptotic spread rate is mainly a function of Re_l**

Size of Liquid Structures

- **Structure Size (per cell at the interface)** $L_{ijk} = \dfrac{2}{|\kappa_{ijk}|}$

Curvature

$$\kappa = \nabla \cdot \vec{n}$$

- **Structure Size PDF :** $prob(L \le L' \le L + dL) = f(L)dL$

$$L_{32} = 2\frac{\Sigma_i P(L_i) L_i^3}{\Sigma_i P(L_i) L_i^2}$$

Not all structures are spherical; more are near-cylindrical. Thus, L_{32} is not exactly the Sauter mean diameter.

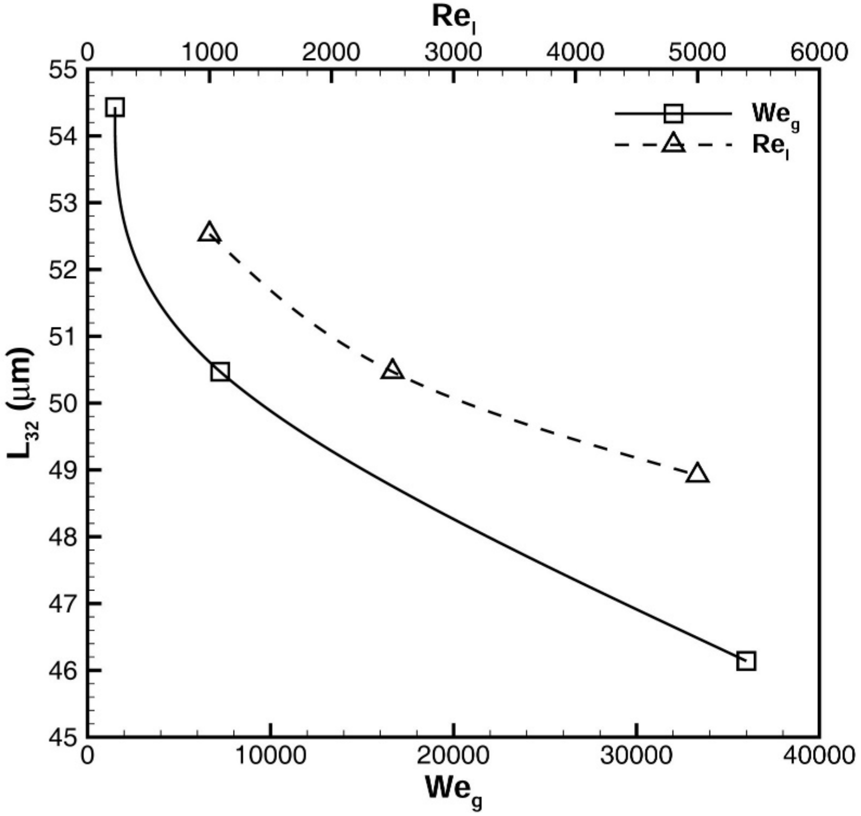

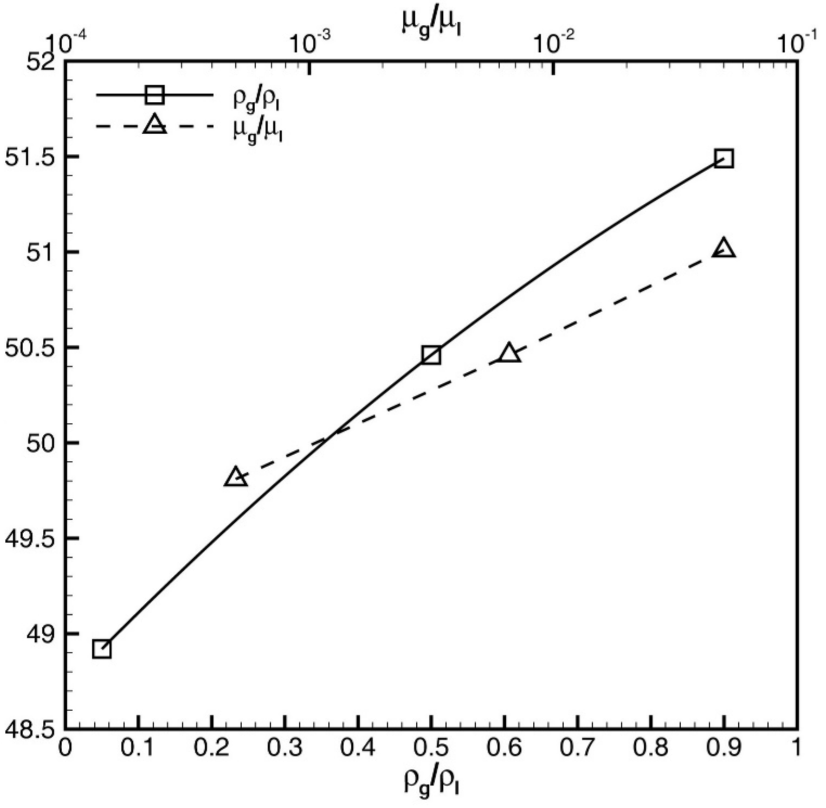

Transcritical Flow Domain

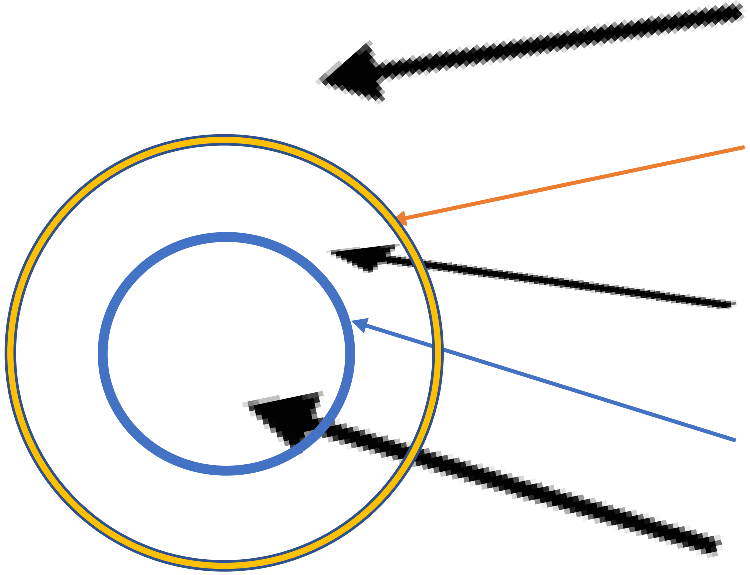

--Outer Domain with Supercritical Fluid

-- Critical Value Interface

--Sub-critical Gas in Annular Domain

-- Droplet Surface

-- Droplet Liquid Interior

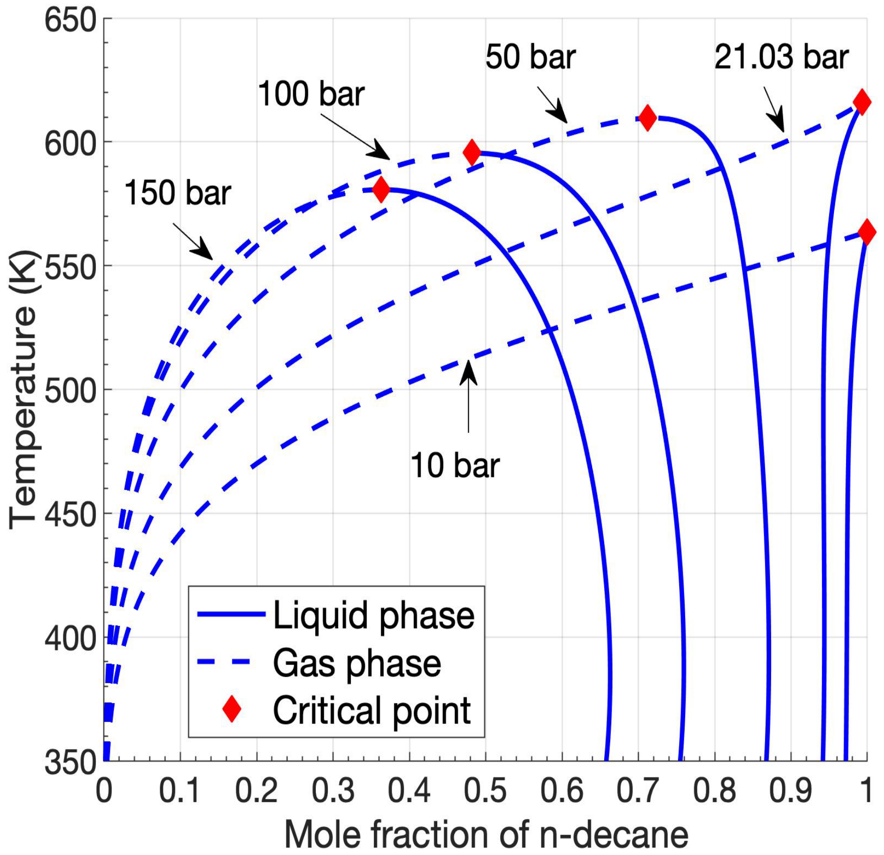

-- Gases easily dissolve in liquids at near-critical conditions.

-- The critical pressure of a multicomponent mixture can be substantially higher than the critical pressure of any component.

-- There are density gradients on both sides of the density discontinuity. A 'fuzzy" experimental image is no proof of supercritical behavior.

Counterintuitive Happenings

- ***Two phases with a sharp interface may exist at a pressure above the critical pressure of all component species. Gas dissolves in the liquid and liquid vaporizes.***
- ***At high pressures, an increasing amount of gas dissolves in the compressible liquid as pressure increases. Thereby, liquid density and liquid viscosity can decrease near the interface with increasing pressure.***
- ***For a hot gas transferring heat by conduction to the cooler liquid at these high pressures, the difference between values of internal energy and enthalpy can be significant. Thereby, in some locations on the interface, there is net condensation rather than net vaporization; the liquid internal energy can exceed the gas value locally because the composition is discontinuous at the interface.***
- ***In the break-up process for a liquid fuel jet at high pressures, small discrete fuel-rich "blobs" appear. The vortex dynamics does cause a non-uniformity of mixture ratio throughout the neighborhood of the liquid-gas interface and penetration of these fuel-rich elements into the oxidizing gas.***

Governing Equations

$$\frac{\partial \rho}{\partial t} + \nabla \cdot (\rho \vec{u}) = 0$$

$$\frac{\partial}{\partial t}(\rho \vec{u}) + \nabla \cdot (\rho \vec{u}\vec{u}) = -\nabla p + \nabla \cdot \bar{\bar{\tau}}$$

$$\frac{\partial}{\partial t}(\rho Y_O) + \nabla \cdot (\rho Y_O \vec{u}) = \nabla \cdot (\rho D_m \nabla Y_O)$$

$F \rightarrow$ Fuel
$O \rightarrow$ Oxidizer
$Y_F + Y_O = 1$

$$\frac{\partial}{\partial t}(\rho h) + \nabla \cdot (\rho h \vec{u}) = \sum_{i=1}^{N} \nabla \cdot \left(\left[\rho D_m - \frac{\lambda}{c_p} \right] h_i \nabla Y_i \right) + \nabla \cdot \left(\frac{\lambda}{c_p} \nabla h \right)$$

Across the interface…

$$\dot{m}'(h_g - h_l) = \left(\frac{\lambda}{c_p} \nabla h \right)_g \cdot \vec{n} - \left(\frac{\lambda}{c_p} \nabla h \right)_l \cdot \vec{n} + \left[\left(\rho D_m - \frac{\lambda}{c_p} \right) (h_O - h_F) \nabla \mathrm{Y_O} \right]_\mathrm{g} \cdot \vec{n} - \left[\left(\rho D_m - \frac{\lambda}{c_p} \right) (h_O - h_F) \nabla \mathrm{Y_O} \right]_\mathrm{l} \cdot \vec{n}$$

KEY ASSUMPTIONS

- Variable fluid properties.
- Fickian diffusion for a binary mixture.
- Low-Mach-number formulation.
- Energy equation rewritten as a transport equation for enthalpy.

Local Thermodynamic Equilibrium

Fugacity

$$f_{gi}(T_g, p_g, X_{gi}) = f_{li}(T_l, p_l, X_{li})$$

$$T_\Gamma = T_g = T_l$$

$$p_g \approx p_l \approx p_{ch}$$

Domain Classification in Terms of Gas Weber Number and Liquid Reynolds Number

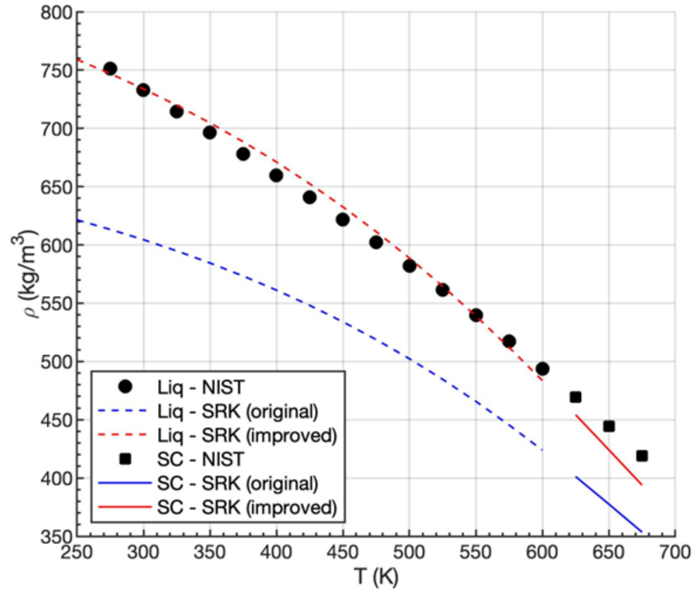

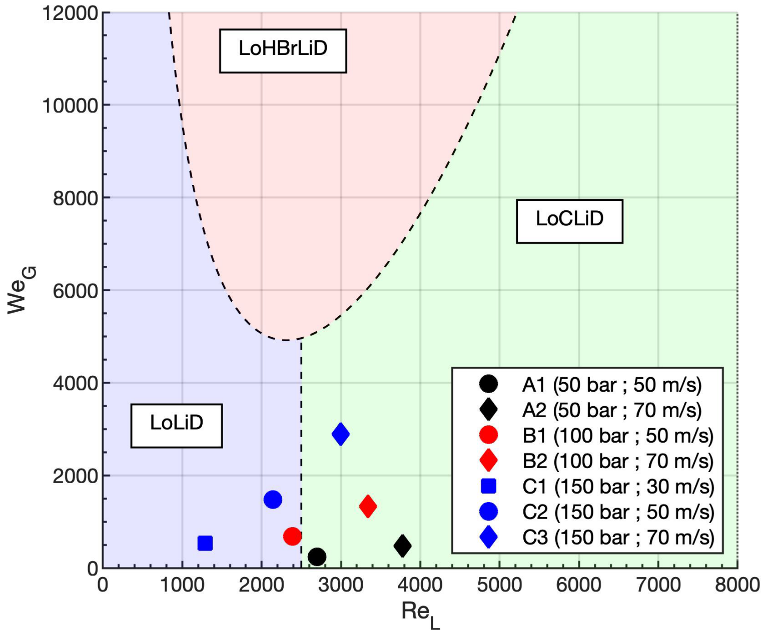

- **Volume-corrected Soave-Redlich-Kwong cubic equation for $Z = pv/(nR_uT)$.**

$$\boxed{p = \frac{R_u T}{v - b + c} - \frac{a}{(v + c)(v + b + c)}}$$

- $\boldsymbol{We_G}$ **and** $\boldsymbol{Re_L}$ **obtained from freestream conditions and an average surface-tension coefficient.**

$$We_G = \frac{\rho_G u_G^2 H}{\sigma} \qquad Re_L = \frac{\rho_L u_G H}{\mu_L}$$

- **How does mixing affect the classification?**

- **What is the role of vortex dynamics?**

Three major paths
-- Lobe Extension, bending, and perforation
-- Lobe and crest corrugation
-- Folding and layering of liquid sheets

MAIN DEFORMATION MECHANISMS

Thermodynamic Pressure \ Relative Velocity or u_G	30 m/s	50 m/s	70 m/s
150 bar	Strong mixing effects. Lobe bending and perforation. Layering of liquid sheets.	Strong mixing effects. Lobe and crest corrugation. Ligament shredding. Layering of liquid sheets.	Strong mixing effects. Lobe and crest corrugation. Ligament shredding. Layering of liquid sheets.
100 bar	-	Mild mixing effects. Lobe bending and perforation. Layering of liquid sheets.	Mild mixing effects. Lobe and crest corrugation. Ligament shredding. Layering of liquid sheets.
50 bar	-	Weak mixing effects. Stronger surface tension. No layering develops.	Weak mixing effects. Stronger surface tension. Lobe stretching but no perforation. Localized liquid sheets.

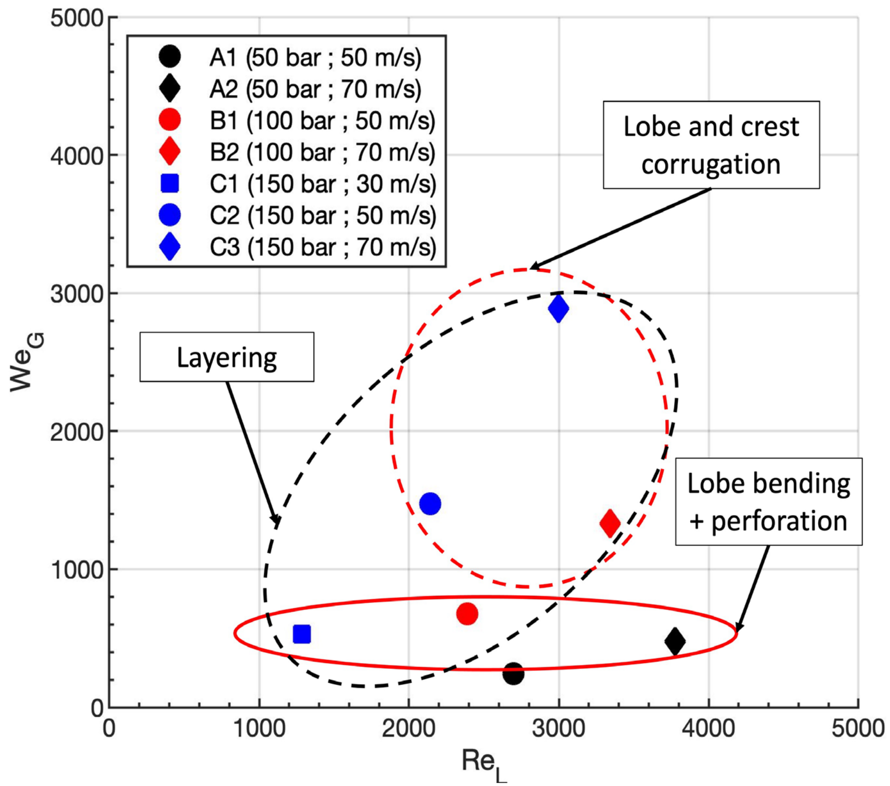

Differences exist with incompressible case even at identical We_g and Re_l.

-- Density gradients

-- Composition gradients

-- Vaporization and condensation

-- Phase equilibrium law

Early Deformation for Lobe Extension, Bending and Perforation Case

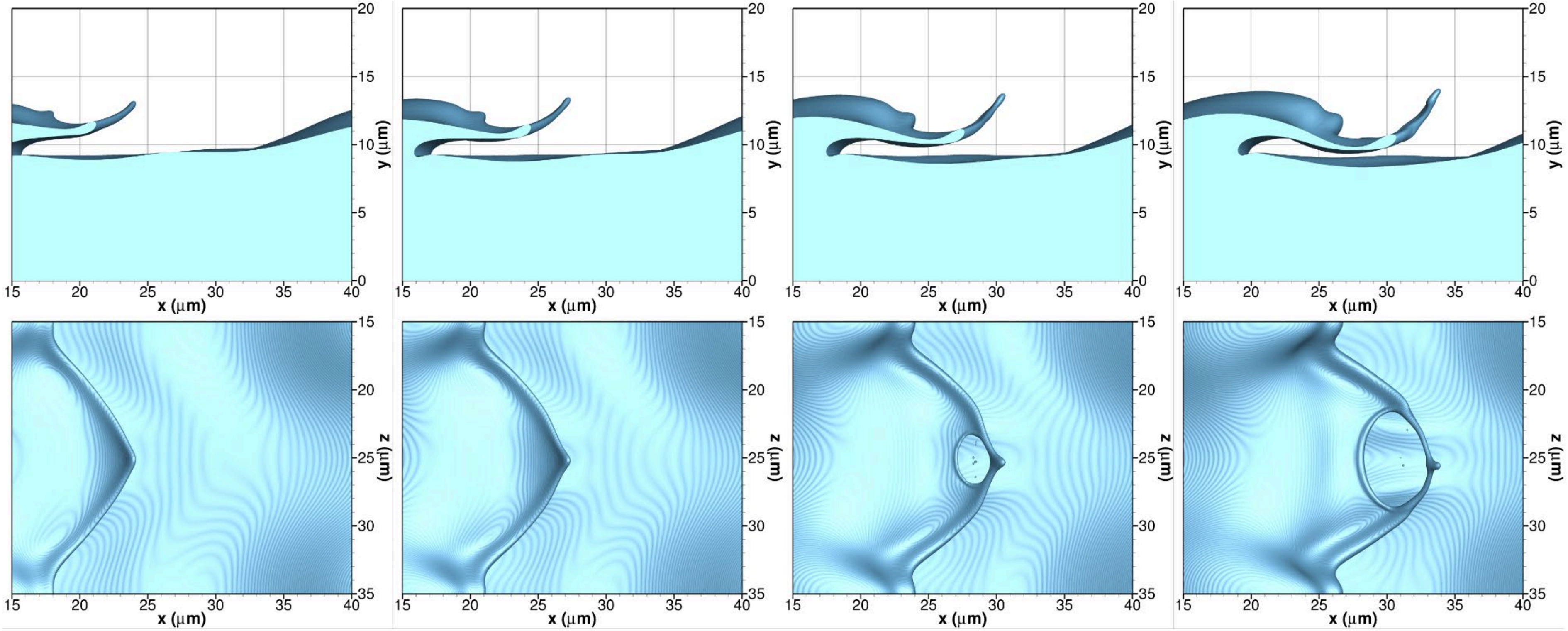

(a) $t^* = 3.75$ (b) $t^* = 4.05$ (c) $t^* = 4.35$ (d) $t^* = 4.65$

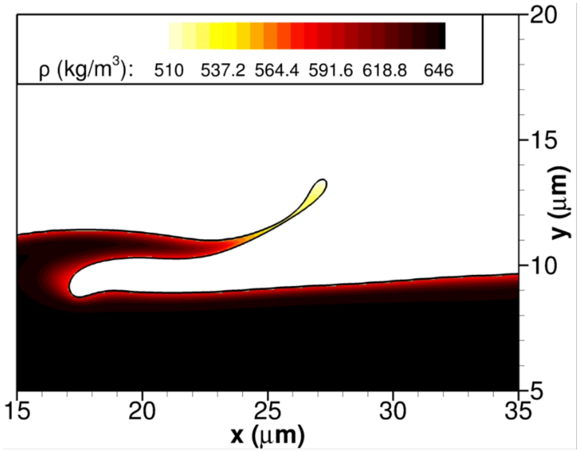

150 bar and $u_G = 30$ m/s
(Case C1)

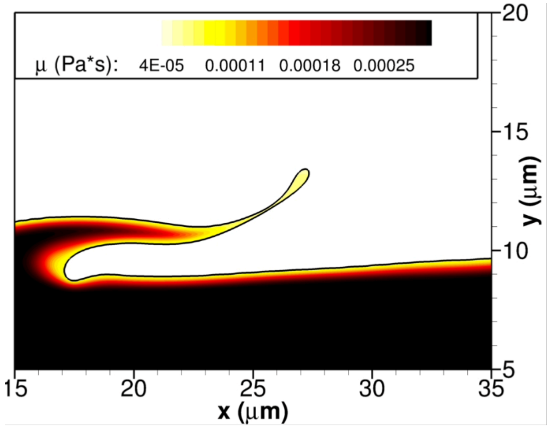

Lobe Extension, Bending and Perforation

- **Before the perforation event…** $\lambda_\rho = -2.5 \times 10^{15}$

150 bar and u_G = 30 m/s (case C1)

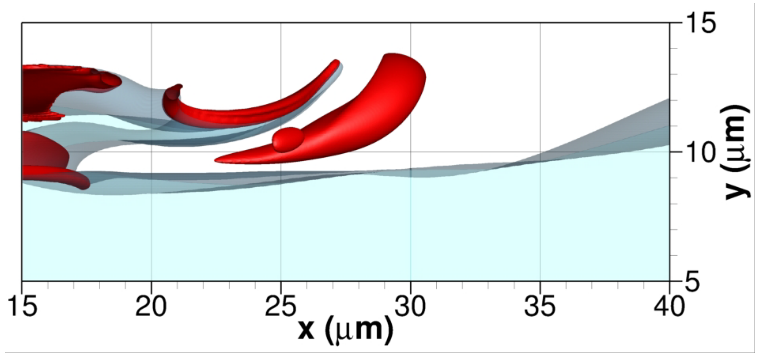

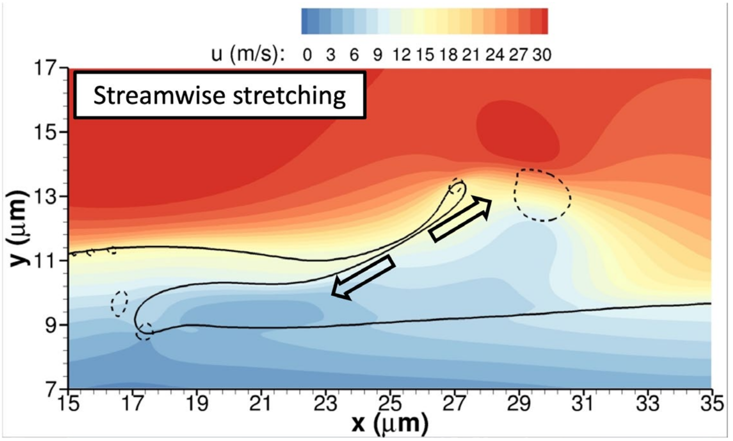

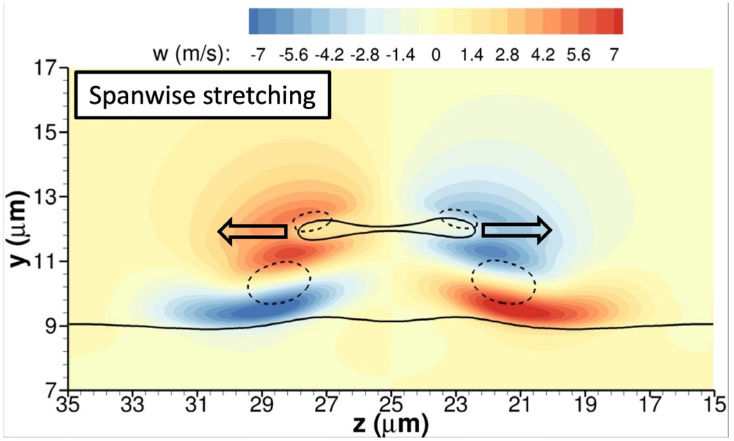

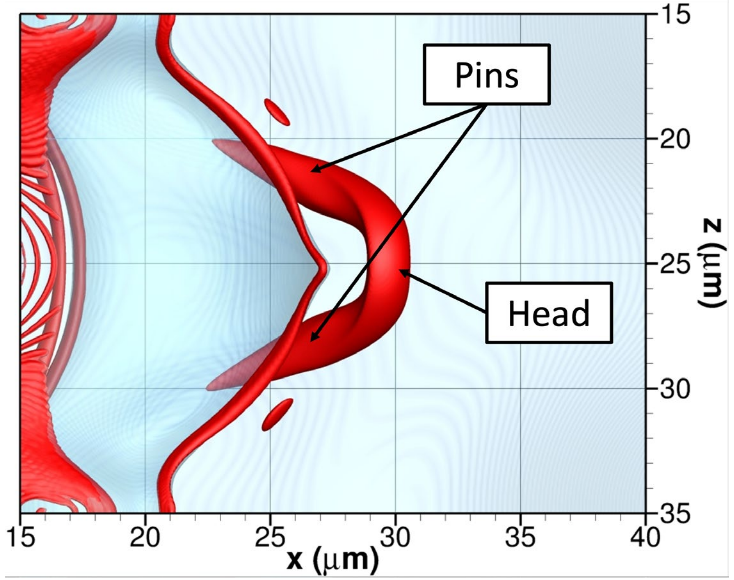

$t^* = 4.05$

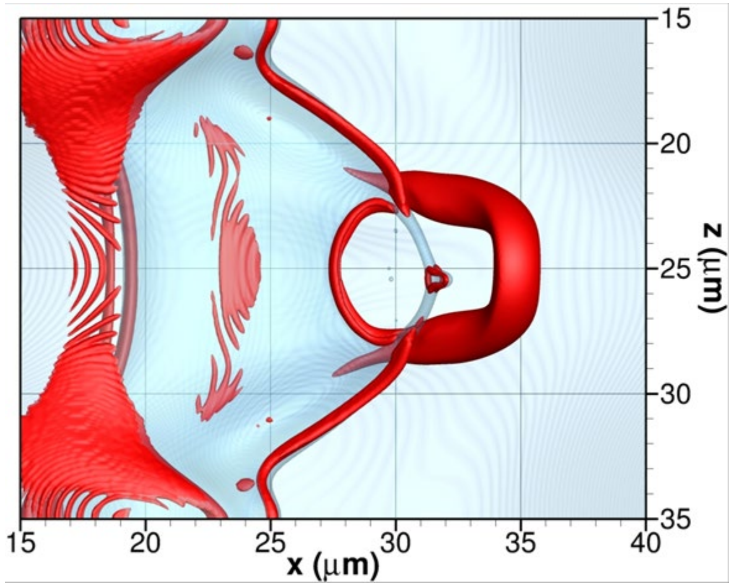

$t^* = 4.50$

- **Two stretching mechanisms are observed.**
- **Lobe thinning occurs.**
- **Hole formation is explained.**

Lobe Extension, Bending and Perforation

Fuel-rich domains form. The domain shapes are determined more by fluid dynamics than by mass diffusion. Disperse "blobs" of fuel are seen.

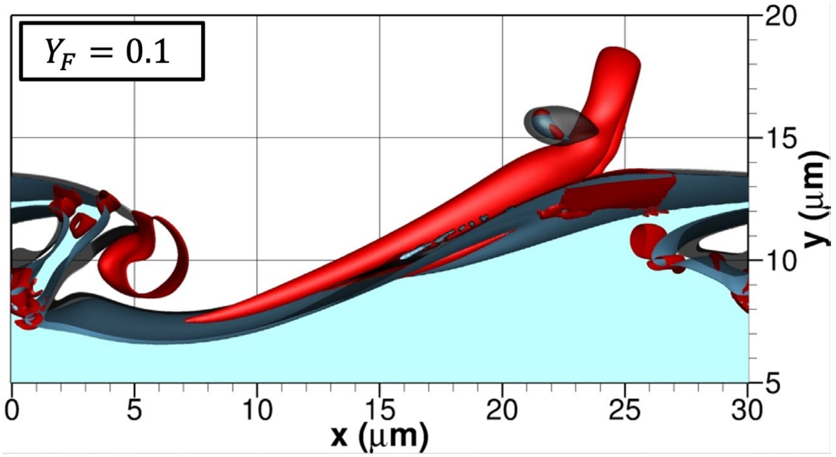

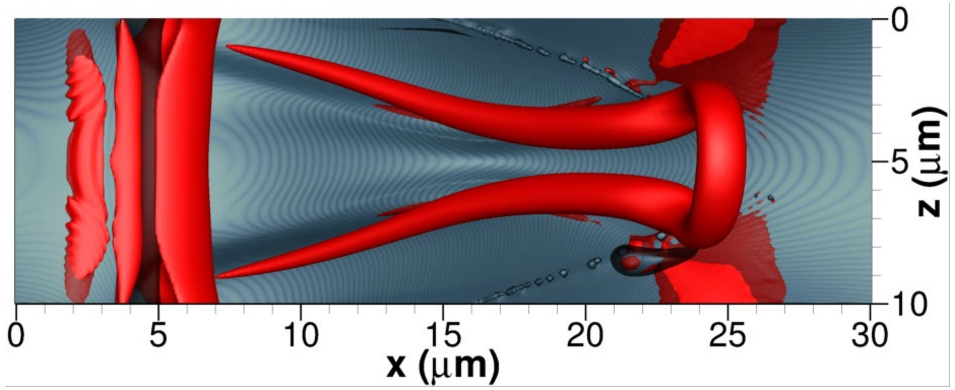

-- Surface Contour for fuel vapor mass fraction YF = 0.1 is shown from three perspectives.

-- Characteristic dimensions of the order of microns are found.

-- These dimensions relate to the dimensions of liquid structures caused by the vortex dynamics.

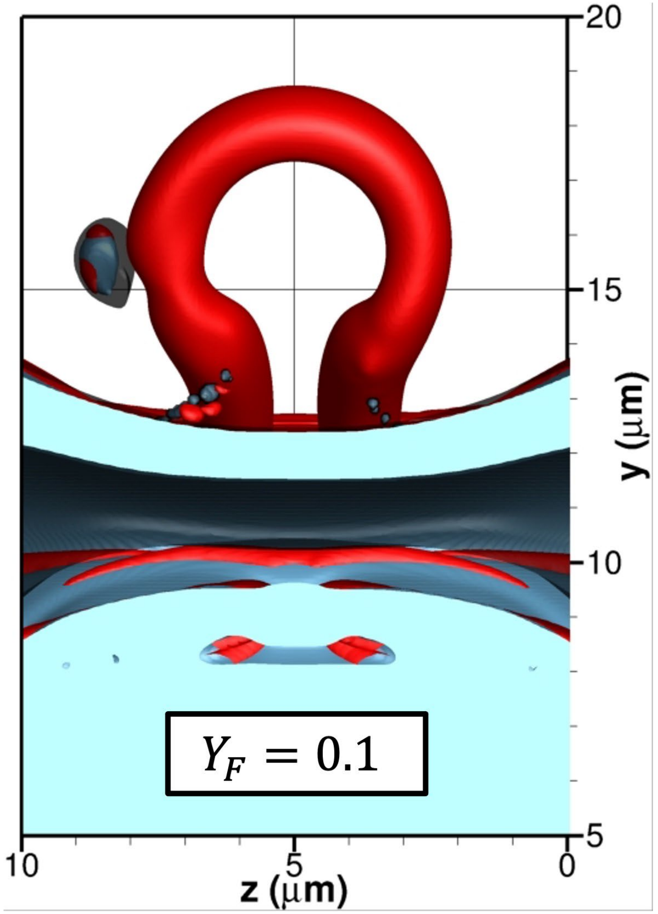

Lobe and Crest Corrugation

- $\lambda_\rho = -9 \times 10^{15}$ kg/(m^{3}s^2)
- Initial roller remains attached.
- Vortex deforms into a hairpin.
- Lobe wraps around the vortex.
- Lobe inflates and bursts.

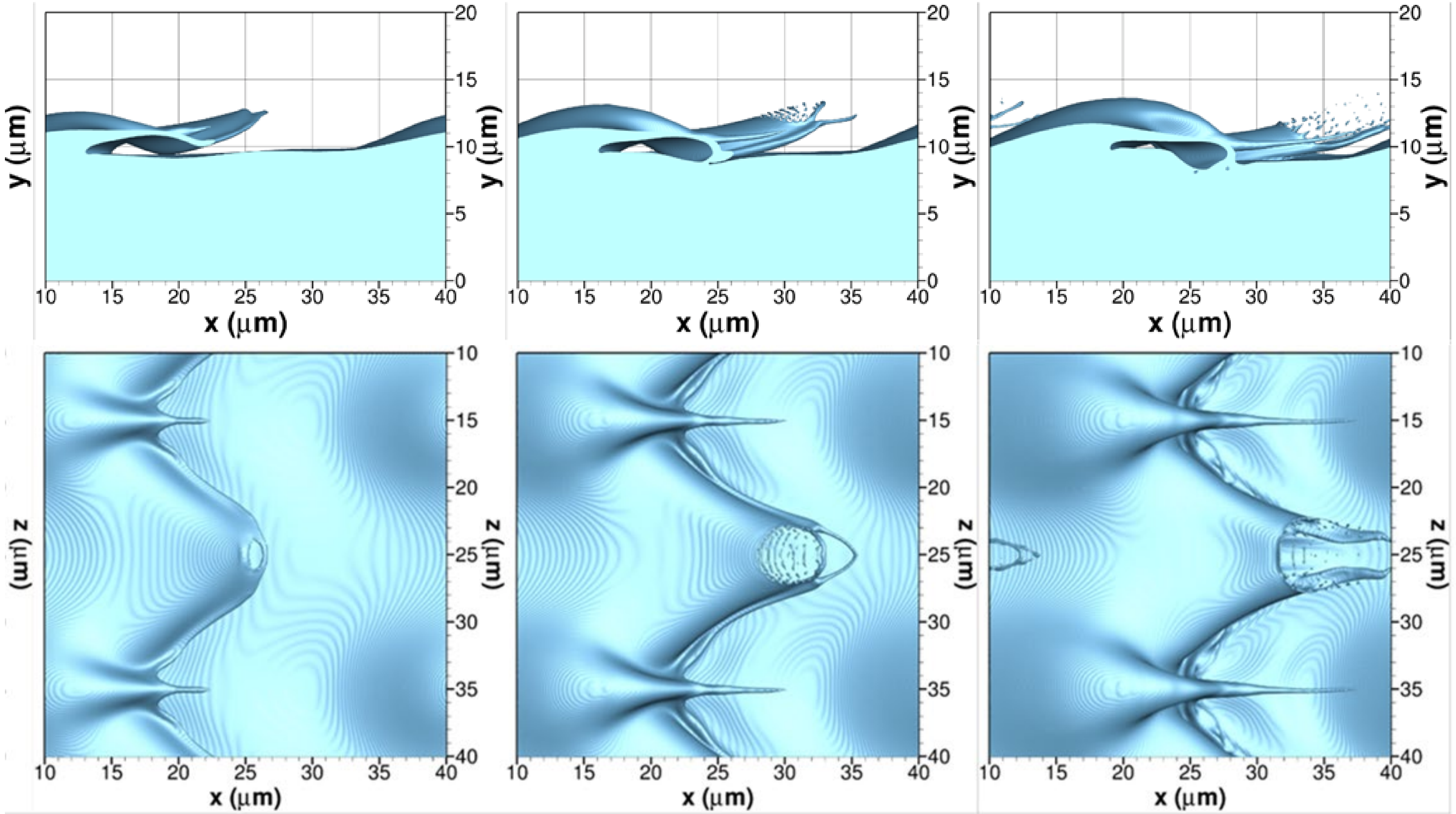

(b) $t^* = 3.5$ (c) $t^* = 4.0$ (d) $t^* = 4.5$

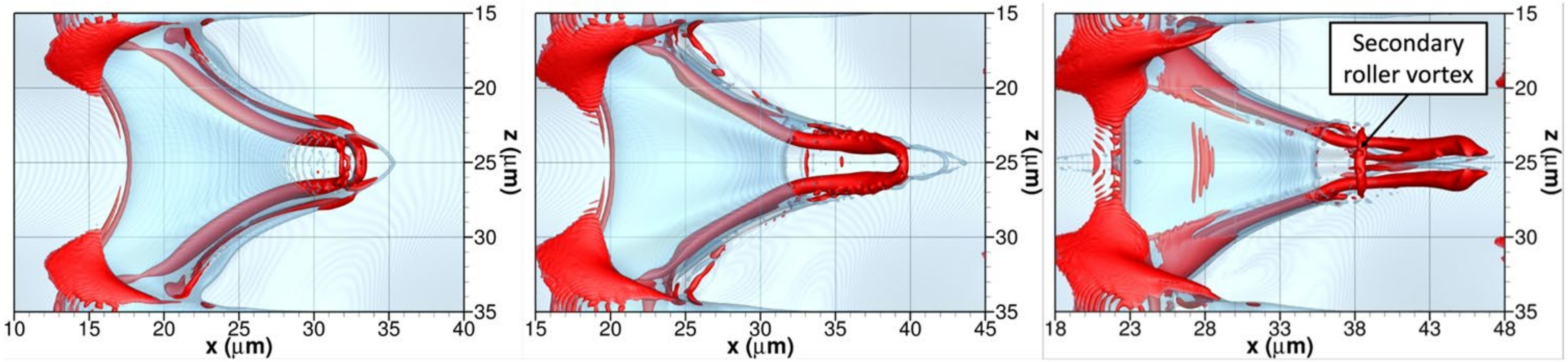

(d) $t^* = 4.00$ (e) $t^* = 4.50$ (f) $t^* = 5.00$

Lobe Corrugation

- **Vortex pins move under the lobe.**

- **The vortex pins stretch the lobe and enhance gas entrainment.**

- **The lobe corrugates and inflates.**

- **The lobe edges merge with the liquid surface below, trapping the vortex pins and ending gas entrainment.**

150 bar and $u_G = 50$ m/s (case C2)

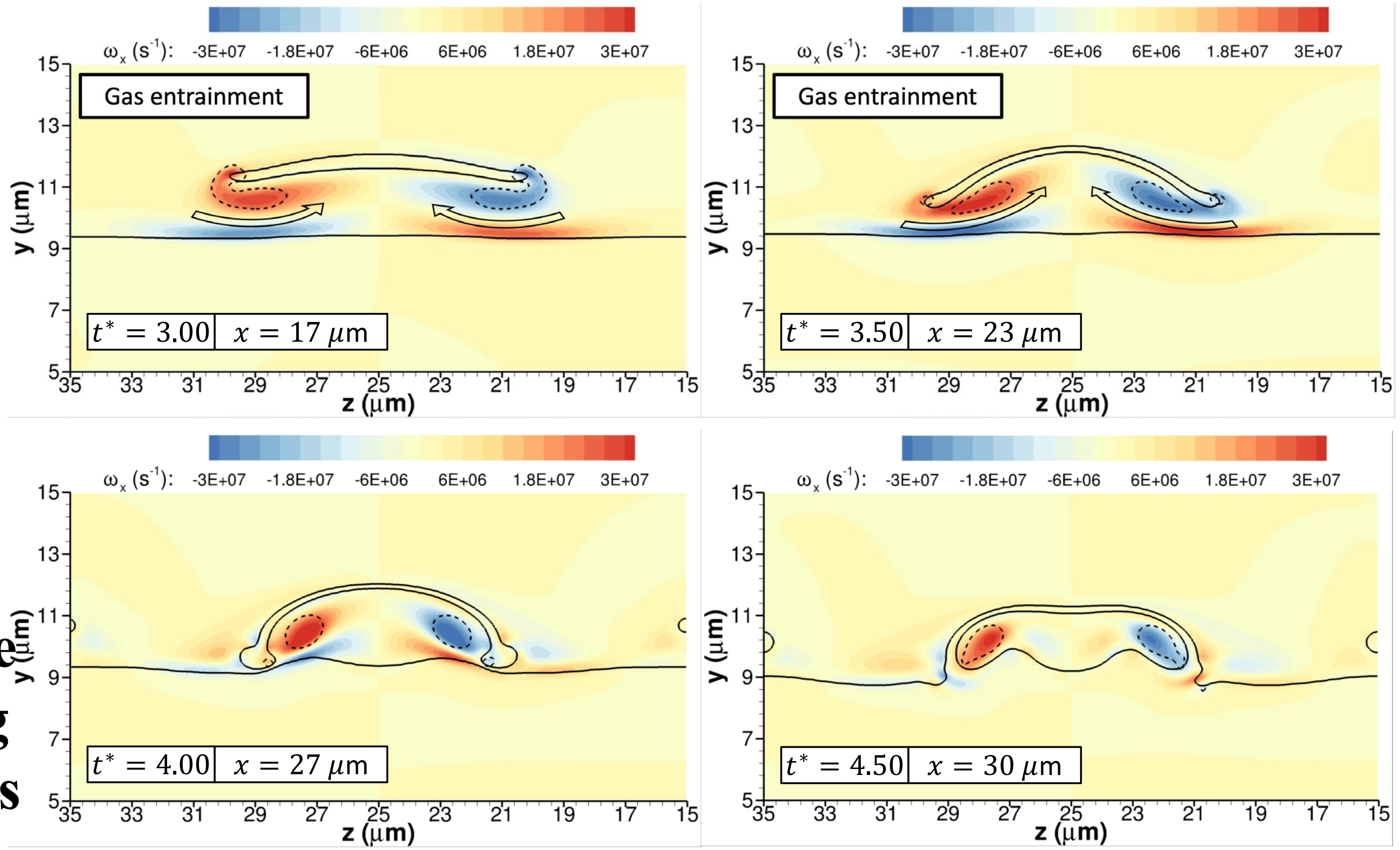

Folding and Layering of Liquid Sheets

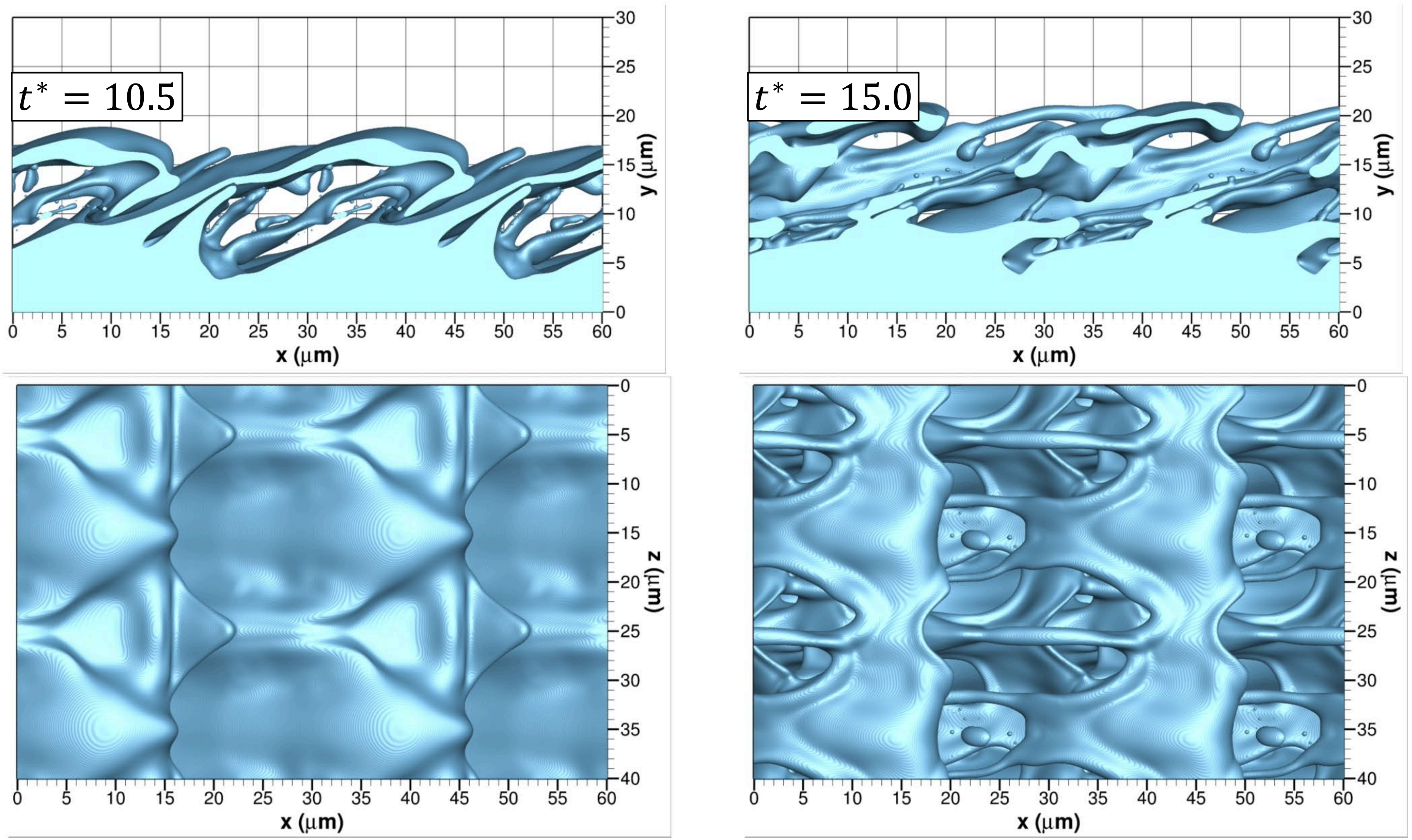

- **Induced by very low surface tension forces + initial shear layer configuration.**
- **Mixing affects the rate of hole formation (e.g., thinner sheets develop) compared to incompressible case.**
- **Higher velocities show ligament shredding and droplet formation.**
- **What implications does layering have?**

150 bar and $u_G = 30$ m/s (case C1)

Folding and Layering of Liquid Sheets

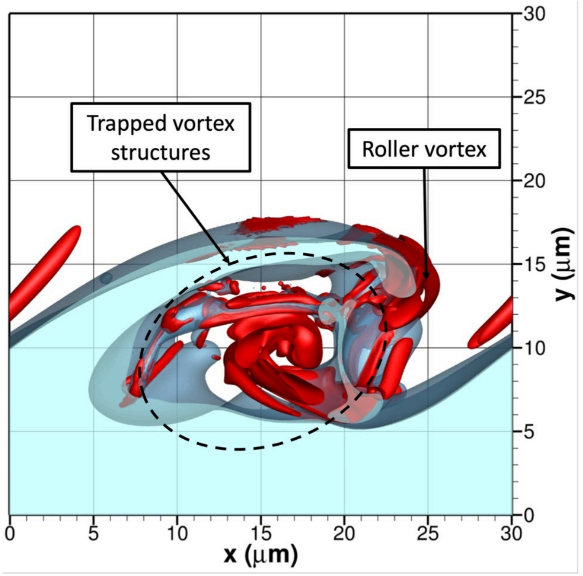

(a) $t^* = 8.40$

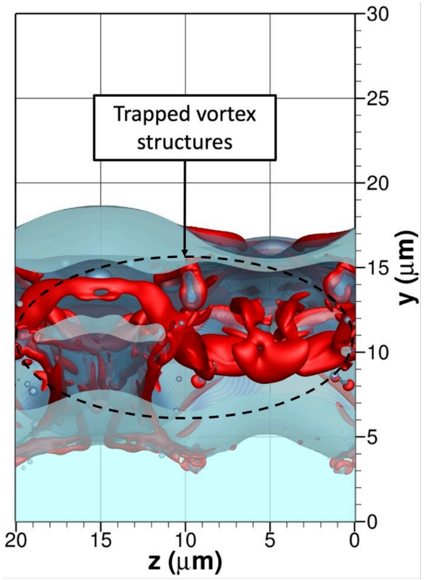

(b) $t^* = 9.90$

150 bar and $u_G = 30$ m/s (case C1)

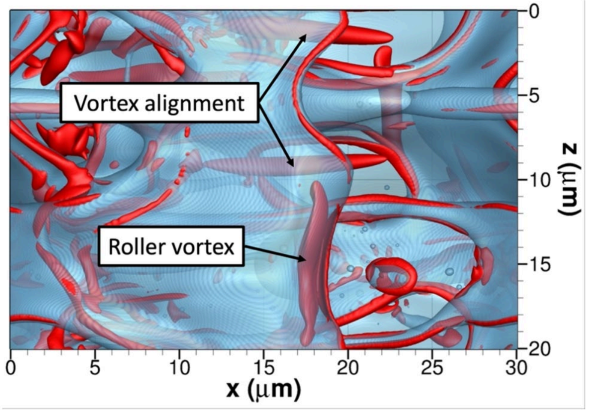

(c) $t^* = 15.00$

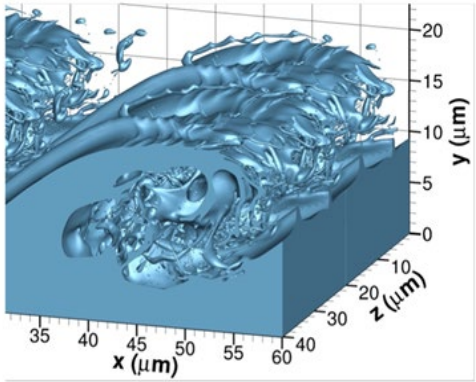

(a) $t^* = 9.625$

100 bar $u_G = 70$ m/s (case B2)

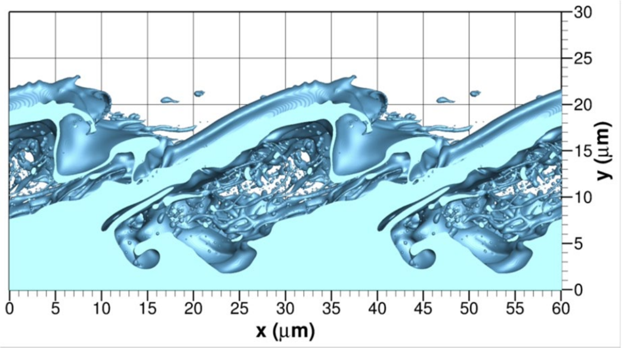

(b) $t^* = 11.55$

- **Induced by very low surface tension forces + initial shear layer configuration.**
- **Thinner sheets develop than for incompressible case.**
- **Short-wavelength instabilities promotes the shredding of ligaments from the wave edge.**

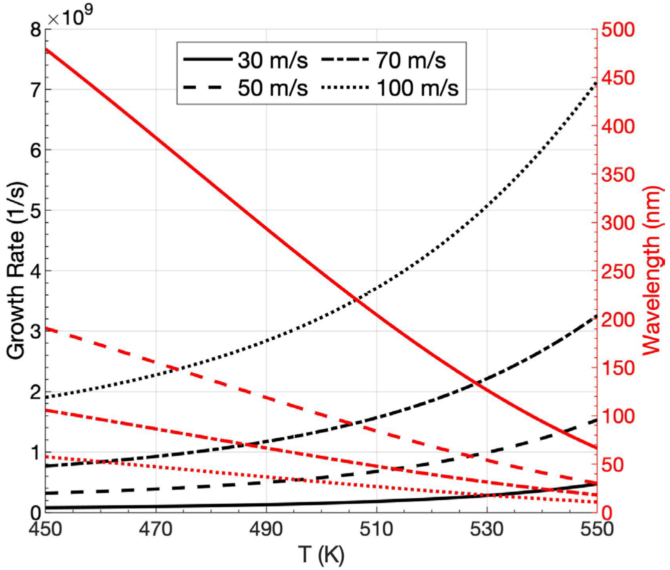

- **Like lobe stretching, mixing causes elongated ligaments.**

Summary

- **Atomization is a cascade process. In particular, it is a form of transitional turbulence.**
- **Accordingly, vortex dynamics can explain the physics of the process.**
- **There are different operational domains with different cascade paths. Reynolds number based on liquid properties and Weber number based on gas properties are key parameters with some importance of density ratio and viscosity ratio.**
- **Two phases with an interface can exist at pressures well above the critical pressure of any involved species. Discontinuities in density and composition occur across the interface and a surface tension exists.**
- **This transcritical atomization can results in counterintuitive behavior: e.g., local condensation with a hotter gas, creation of fuel-rich "blobs" through the oxidizing gas through atomization of a liquid fuel jet.**

Thank you.

-- D. Jarrahbashi and W. A. Sirignano, "Vorticity Dynamics for Transient High-Pressure Liquid Injection,", invited paper, *Physics of Fluids* 26 (10), 101304, 2014. Based on Invited Lecture at APS Meeting.
-- D. Jarrahbashi, P. P. Popov, W. A. Sirignano,, and F. Hussain, "Early Spray Development at High-Density: Hole, Ligament, and Bridge Formations," *Journal of Fluid Mechanics* 792, pp. 188-231, 2016.
-- D. Jarrahbashi, P. P. Popov, W. A. Sirignano, and F. Hussain, "Numerical Simulation of Liquid Round Jet Atomization," *Physical Review Fluids*, invited paper, 2, 090504, 2017.
-- A. Zandian, W. A. Sirignano, and F. Hussain, "Planar Liquid Jet: Early Deformation and Atomization Cascades," *Physics of Fluids* 29, 062109, 2017.
-- Zandian, W. A. Sirignano, and F. Hussain, "Understanding Liquid Jet Atomization Via Vortex Dynamics," *Journal of Fluid Mechanics* 843, pp. 293-354, 2018.
-- J. Poblador-Ibanez and W. A. Sirignano, "Transient Behavior near Liquid-Gas Interface at Supercritical Pressure," *International Journal of Heat and Mass Transfer* 126, Part B, pp. 457-73, 2018.
-- Zandian, W. A. Sirignano, and F. Hussain, "Length-scale Cascade and Spray Expansion for Planar Liquid Jets," *International Journal of Multiphase Flow* 113, pp.117-41, 2019.
-- Zandian, W. A. Sirignano, and F. Hussain, "Vorticity Dynamics in a Spatially Developing Coaxial Liquid Jet inside Gas Flow," *Journal of Fluid Mechanics* 877, pp. 429-70, 2019.
-- J. Poblador-Ibanez, B.W. Davis, and W. A. Sirignano, "Self-similar Solution of a Supercritical Two-phase Laminar Mixing Layer", *International Journal of Multiphase Flow* 135, Article 103465, 2021.
-- B.W. Davis , J. Poblador-Ibanez, and W. A. Sirignano, "Two-phase Developing Laminar Mixing Layer at Supercritical Pressures," *International Journal of Heat and Mass Transfer* 167, Article 120687, 2021.
-- J. Poblador-Ibanez and W. A. Sirignano, "Liquid-jet Instability at High Pressures with Real-fluid Interface Thermodynamics", *Physics of Fluids*, 33, 083308, 2021.
-- J. Poblador-Ibanez and W. A. Sirignano, "Temporal Atomization of a Transcritical Liquid n-decane Jet into Oxygen," *International Journal of Multiphase Flow* 153, 104130, 2022.
-- J. Poblador-Ibanez and W. A. Sirignano, "A Volume-of-Fluid Method for Variable-density, Two-phase Flows at Supercritical pPressure", *Physics of Fluids* 34, 053321, 2022.
-- J. Poblador-Ibanez,W. A. Sirignano, and F. Hussain, "Role of Vorticity Dynamics for Transcritical Liquid Jet Breakup," in preparation, 2022.

Instabilities

INTRODUCTION

Kelvin-Helmholtz (KH)

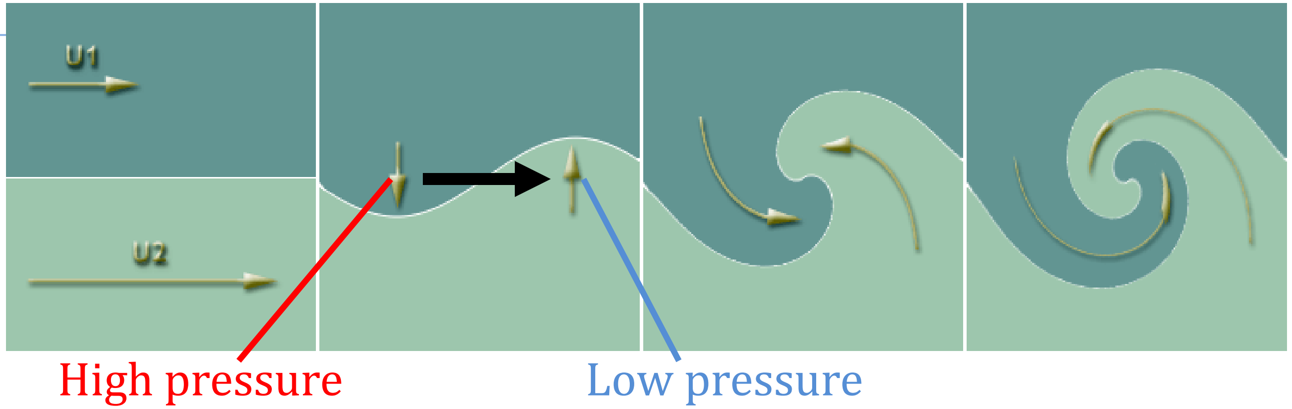

Rayleigh-Taylor (RT)

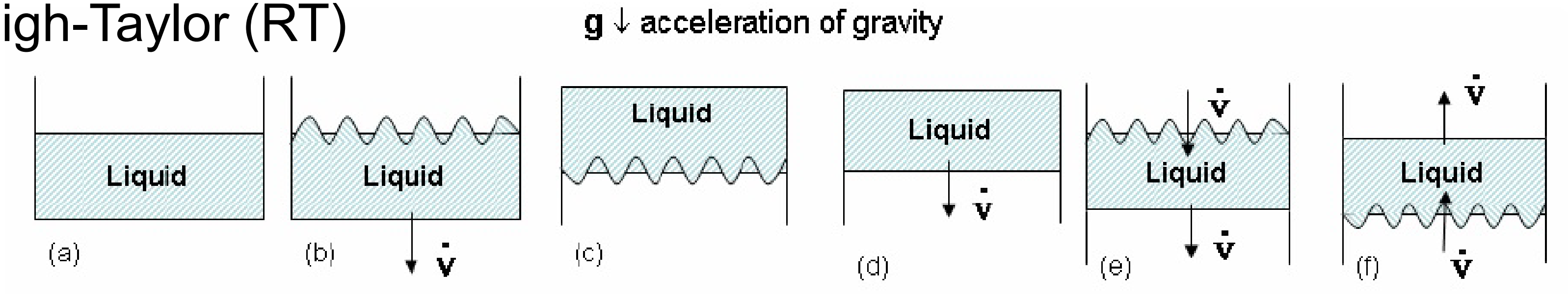

Capillary (Rayleigh) instability

R_2 is negative at the trough and positive at the crest

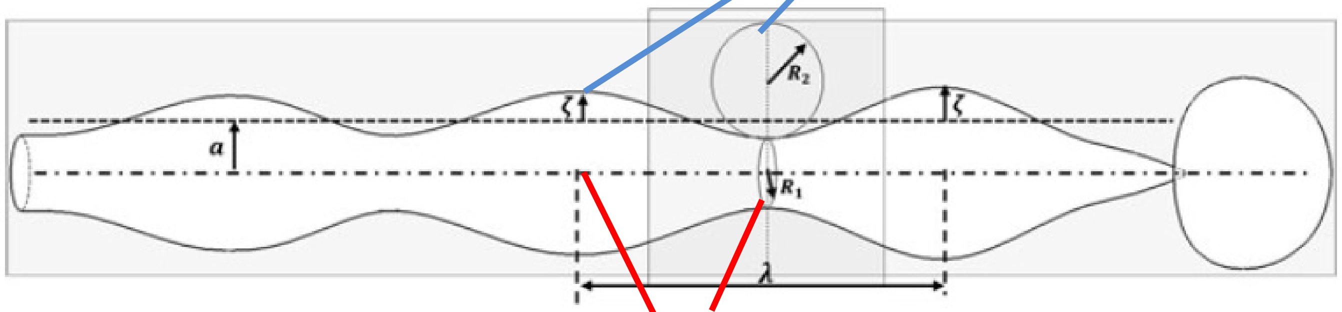

R_1 at the trough < R_1 at the crest

If $\lambda > 2\pi R_1 \rightarrow$ Unstable

Planar jets show a similar character regarding liquid structures; lobes, holes, bridges, ligaments, droplets

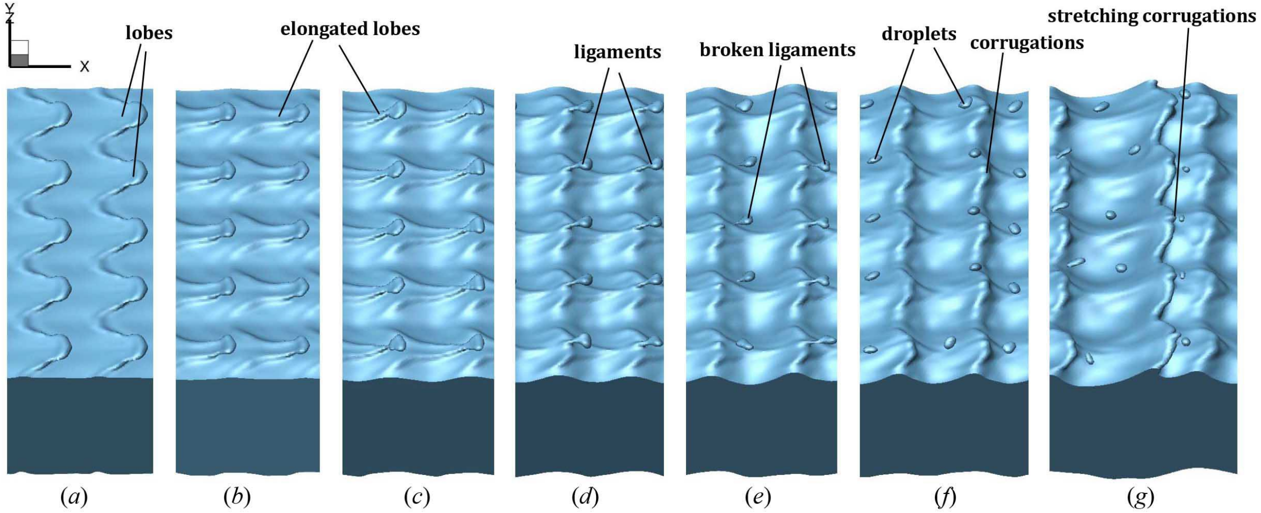

Early deformations: character depends on Re, We, density ratio.

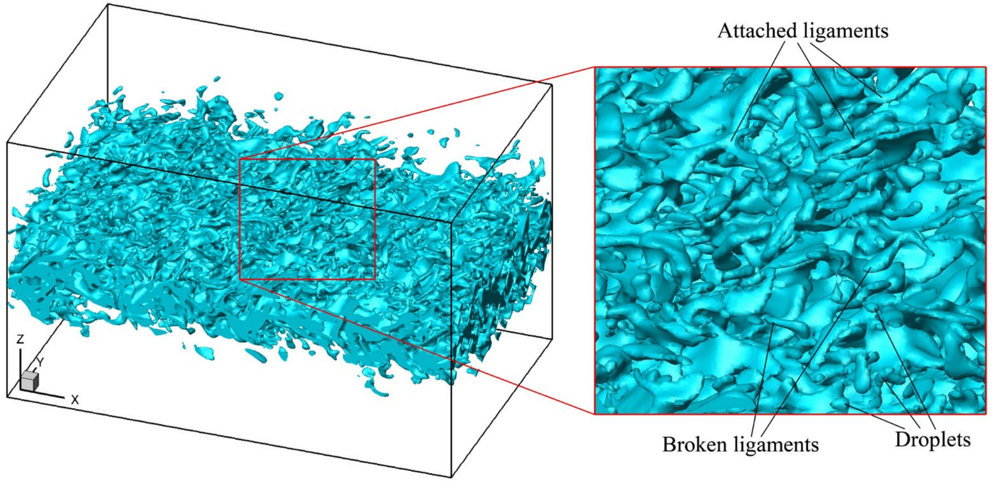

Deformation at later time.

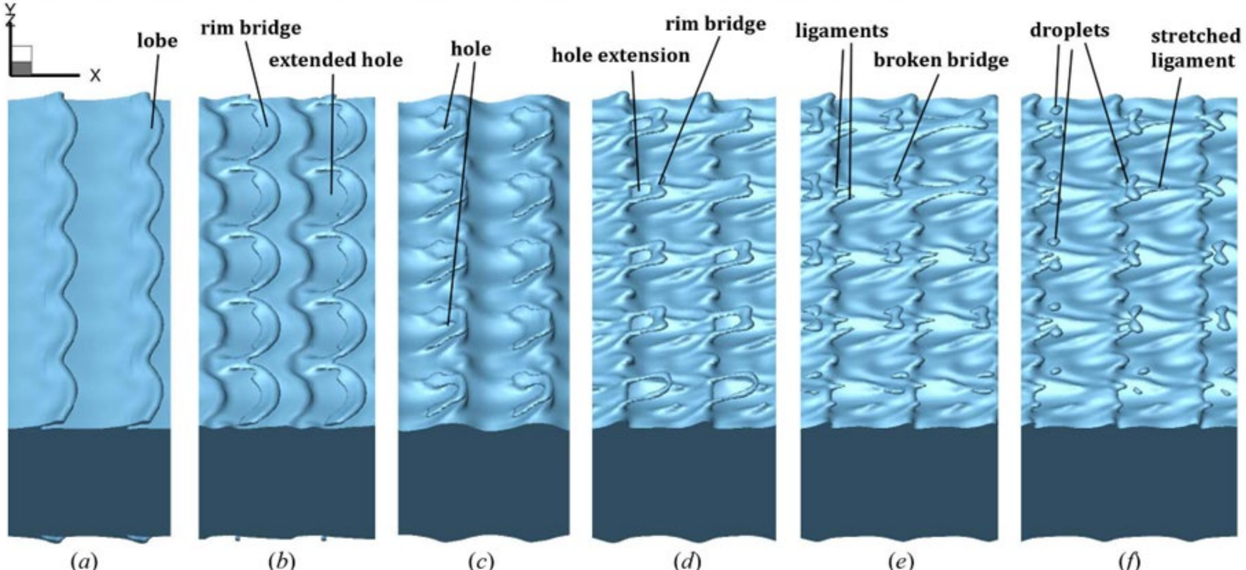

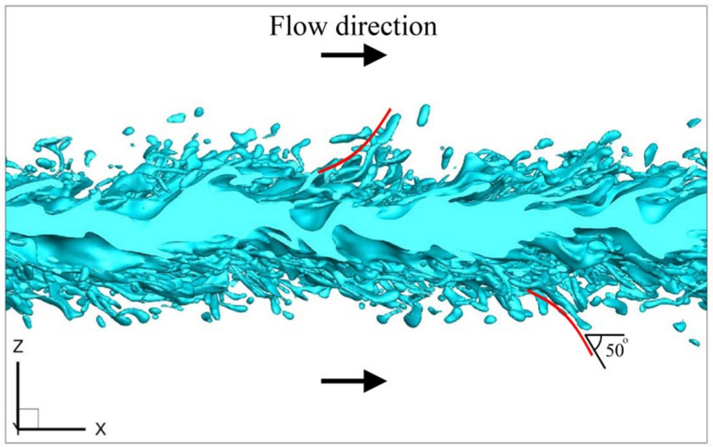

(a)

Spray angle, inferred from temporal analysis,

increases by decreasing Re_l, by increasing We_g, and by increasing $\hat{\rho}$, while not much affected by $\hat{\mu}$